Research article

Integrated molecular analyses of an interferon-γ based subtype with regard to outcome, immune characteristics, and immunotherapy in bladder cancer and experimental verification

Jirong Wang, Siyu Chen, Huabin Wang, Jinlong Cao, Xinpeng Fan, Jiangwei Man, Qingchao Li, Li Yang [*]

Department of Urology, The Second Hospital of Lanzhou University, Lanzhou, Gansu, People's Republic of China

A B S T R A C T

This study attempted to explore the role of interferon-γ related genes (IRGs) in the prognosis and immunotherapy of bladder cancer (BC). Based on data downloaded from public databases, molecular subtypes with different IRG expression patterns were determined via nonnegative matrix factorization clustering. On the basis of IRGs, interferon-γ related gene signature (IRGS) was developed through Cox regression analyses. We identified that two molecular subgroups with different outcome and immune profiles. It was proved that IRGS possessed prediction efficiency for BC prognosis. Compared with low IRGS group, high IRGS group was related to less anti-cancer immune cells infiltration, less tumor mutation burden score, more cancer stem cell index, and less benefit from immunotherapy. Differential expression of six model genes (*IRF5, LATS2, MTHFD2, VAMP8, HLA-G* and *PTPN6*) was validated between paired tissues by RT-qPCR. This study presents a prognostic model, which could serve as an indicator for the benefit of BC immunotherapy.

1. Introduction

Bladder cancer (BC) is one of most shared types of urologic cancers and the ninth most lethal malignant tumor [1]. It is estimated that nearly 550000 new individuals were diagnosed with BC across the world per year, resulting in approximately 200000 deaths annually [2]. Recent studies have demonstrated that more than 40% of muscle-invasive BC patients were inoperable when diagnosed [3, 4]. Despite substantial progress has been made in early diagnosis and novel therapeutic interventions, clinical outcomes of BC patients are still not satisfactory [5]. Thus, there is an urgent need to improve risk stratification and the rate of early diagnosis of BC. Conventional treatment modalities for BC include surgery, radiotherapy, and chemotherapy [6, 7]. In the past decades, despite the optimal treatment of surgical resection, the five-year survival rate of late-stage BC patients is still less than 50% [8, 9]. For advanced bladder cancer, traditional therapies of BC including radiotherapy and chemotherapy incapable of controlling tumor progression effectively [10, 11, 12]. Immunotherapy based on immune checkpoint inhibitors (ICI) such as targeting PD-1,PD-L1, and CTLA4 as an option could fulfill this unmet need, and has shown favorable oncological outcomes in

advanced BC patients [13]. Further, ICI have demonstrated efficacy in various kinds of cancers including BC [14, 15]. However, a number of BC patients treated with immunotherapy do not experience clinical benefit due to the clinical response rates are far from sufficient [16]. Hence, how to evaluate the response of BC patients to ICI is still a problem to be solved.

The tumor microenvironment (TME) consists of tumor cells, stromal cells, cytokines, immune cells and other components. Increasing evidences have demonstrated that different subpopulations of infiltrating immune cells in the TME is associated with the outcome of patients and the abundance of infiltrating immune cells could affect the response of patients to ICI therapy [17, 18]. For instance, previous studies demonstrated that infiltrating regulatory T cells-induced suppressive tumor microenvironment is a critical obstacle for effective tumor immunotherapy [19]. Some reports pointed out that PD-L1 expression levels and abundance of CD8 T cells infiltrated in the TME could influence interindividual differences in immune checkpoint inhibitors response [20, 21, 22]. More specifically, a clinical experiment proved that patients with dense CD8+T cells infiltration show higher responsivity to pembrolizumab [23]. In addition, recent study has also suggested that

mucosal melanoma patients with sparse lymphocytes infiltration tend to benefit less from ICI therapy [24]. To some extent, the tumor immune microenvironment (TIME) is the underpinnings of ICI therapy, understanding the immune cells infiltration profile in the TME is the cornerstones of developing effective precision ICI therapy strategy [25].

Interferon gamma (IFN-γ) as a pleiotropic cytokine, is a complex regulator of the TIME and participates in the coordination of tumor-related immune response [26]. On the one hand, IFN-γ secreted by T cells and natural killer (NK) cells could suppress cancer cells growth via tumor-infiltrating macrophages recruitment and cytotoxic T-cell proliferation activation [27, 28]. On the other hand, IFN-γ is also an essential contributor to the demotion of antitumor immune responses [29]. Specifically, IFN-γ secreted by lymphocytes can induce the upregulation of immune checkpoints expression (PD-L1, PD-L2) within the TIME, thus mediating tumor immune escape [30, 31]. Afterwards, it was reported that activation of interferon stimulated genes was closely related to both superior prognosis and inferior prognosis following ICI therapy [32]. Furthermore, previous studies indicated that the IFN-γ related genes model enables prediction of prognosis and ICI therapy benefit for clear cell renal cell carcinoma and lung adenocarcinoma [33, 34]. Some retrospective studies also demonstrated that the expression levels of interferon gamma showed tight correlation with the outcome of BC patients [35, 36]. With the rapid development of high-throughput sequencing, the research of molecular signatures in tumor has shown a promising prospect. Nevertheless, no studies have involved comprehensive bioinformatic analysis or identification of IFN-γ related genes as risk model focused on both the outcome and immunotherapy benefit for BC. Moreover, there were also few biomarkers of BC can effectively predict prognosis and guide therapy [37]. Thus, this article aims to identify the molecular subgroups on the basis of different interferon-γ related genes expression patterns via NMF clustering, and develop an interferon-γ related gene signature (IRGS) associated with the TIME to facilitate the molecular stratification of BC and maximize the benefits of ICI therapy. The process flowchart of the research was summarized in Fig. S1.

2. Materials and methods

2.1. Datasets collection

RNA-seq data and clinical data regarding 412 BC and 19 normal bladder tissue samples were mined from TCGA database, and the 165 GEO BC samples with complete survival data were obtained from microarray data of GSE13507(Table S1). The IMvigor210 cohort of 208 metastatic urothelial tumor patients treated with anti-PD-L1 therapy was chosen to confirm the IRGS prediction ability of clinical benefit from ICI therapy (http://research-pub.gene.com/IMvigor210CoreBiologies/). Then, IFN-γ related genes were extracted from the gene set "HALLMARK_INTERFERON_GAMMA_RESPONSE" (https://www.gsea-msigdb.org/). Also, copy number variation (CNV) data and the TCGA cohort corresponding survival data (overall survival, disease-free survival, disease-specific survival and progression-free survival) was obtained from UCSC Xena database (https://xenabrowser.net/). The reported BC immune classifications data and gene mutation information were also acquired from TCGA databases [38]. The cancer stem cell (CSC) index of BC was used to describe the similarity between tumor cells and stem cells, and the CSC index data was obtained from the study of Malta et al. [39].

2.2. Screening of differentially expressed genes and preliminary classification

First, referring to the RNA-seq data of TCGA BC samples, differentially expressed IFN-γ related genes between normal and tumor tissues were determined (criteria were $p < 0.05$ and $|log2FC| > 0.585$). Then, functional analyses (GO and KEGG) based on these genes was performed. Protein-Protein Interaction (PPI) analysis of differentially expressed IFN-

γ related genes was performed using the STRING website (http://string-db.org). Moreover, we also assessed somatic copy number alterations in these differentially expressed IFN-γ related genes. Second, based on differentially expressed genes, nonnegative matrix factorization (NMF) clustering was conducted to identify the molecular subgroups by the R package "NMF". Third, the immune composition, purity, and immunocytes infiltrated profile of each sample were calculated via the ESTIMATE and the microenvironment cell-population (MCP)-counter algorithms. Finally, principal components analysis (PCA) was performed using the R package "PCA".

2.3. Construction and validation of a prognostic signature based on IRGS

Univariate Cox regression analysis was used to screen prognostic genes from differentially expressed genes. Based on this, multivariate Cox regression analysis was performed to construct the IRGS, and the model was finalized using following formula: risk score $= \sum_{i=1}^{n} exp(i) * coef(i)$ where exp represented the gene expression value while coef represented the coefficient. Then, BC patients were subdivided into the high and low IRGS groups using the criterion of median risk score. Kaplan-Meier (K-M) survival analysis was conducted to compare the overall survival (OS), disease-free survival (DFS), disease-specific survival (DSS) and progression-free survival (PFS) between the high and low IRGS groups. Univariate and multivariate Cox regression analyses were applied to evaluate whether the IRGS possessed independent prognostic value. The receiver-operating characteristic (ROC) curves were generated to measure the diagnostic efficacy of IRGS. Finally, we analyzed the correlation between IRGS scores and clinical features.

2.4. Development and validation of the nomogram based on the IRGS

Nomogram for OS of BC prediction was developed based on the clinical features and the IRGS. Moreover, calibration curves were implemented to evaluate the calibration of the nomogram. Also, concordance index (C-index) and ROC curves were applied to assess the discriminating superiority of nomogram.

2.5. Identification molecular and immune characteristics of IRGS subgroups

First, to probe the relationship between the eight genes and OS, we conducted K-M analysis on the identified genes. Second, to further explore the potential function of the eight genes, the Gene Set Enrichment Analysis (GSEA) based on the KEGG gene set (c2. cp.kegg.v7.4. symbols.gmt) and Gene ontology (GO) enrichment analysis were performed (NOM $p < 0.05$ and false discovery rate (FDR) < 0.05). Third, for evaluation of immune and molecular response among the IRGS subgroups, immune cell infiltration and some cancer-associated pathways (extracted from gene set h. all.v7.4. symbols.gmt) were estimated via the CIBERSORT algorithm and Gene Set Variation Analyses (GSVA) [40]. Meanwhile, correlation analysis was applied to screen the relevance between immunocyte infiltration and risk scores with the Pearson correlation analysis. Finally, we explored the relationships between the IRGS and tumor mutation burden (TMB) score and CSC index.

2.6. Prediction of ICI therapy response

The data of BC patients ICI therapy efficacy was downloaded from The Cancer Imaging Archive (TCIA, https://tcia.at/). Then, the IMvigor210 cohort was chosen to validate the IRGS prediction ability of clinical benefit from ICI therapy. Furthermore, the T-cell dysfunction and exclusion gene expression (TIDE) and tumor inflammation signature (TIS) signatures scores were calculated as the normalized expression of genes provided by original article [41, 42]. Besides, the ROC curves and

C-index were generated to measure the diagnostic value of IRGS, TIS, and TIDE.

2.7. Investigation of drug sensitivity

To assessed the IRGS prediction ability of sensitivity to chemotherapeutic agents and potential drugs, we estimated the half-maximal inhibitory concentration (IC_{50}) of the commonly-used chemotherapeutic agents and potential drugs for BC through the R package pRRophetic. The Wilcoxon signed-rank test was conducted to analyze IC_{50} difference among the IRGS subgroups.

2.8. Specimen collection and RT-qPCR

A total of four paired BC tissues (C1, C2, C3, C4) and adjacent noncancerous tissues (N1, N2, N3, N4) were collected from the Second Hospital of Lanzhou University between January and March 2022 (detailed clinical data of the patients can be found in Table 1). All tissues were confirmed by two independent pathologists. Tissue samples were immediately frozen and stored at -80 °C for further analysis. Based on manufacturer' s protocol, Trizol (Takara) was used to extract total RNA in tissue samples. cDNA was produced by total RNA using a PrimeScript™ RT reagent kit (Perfect Real Time; Takara). Primer was synthesized by Tsingke Biological Technology (Beijing, China) and the sequence as suggested in following table (Table S2) Reverse transcription-quantitative PCR (RT-qPCR) was performed by Bio-Rad CFX96 real-time PCR detection system (Bio-Rad, Hercules, California, USA). β-actin serve as the internal control, and all operations were repeated 3 times. Relative expression levels of genes were analyzed by the $2^{-\Delta\Delta Ct}$ method. Meanwhile, we also explored the protein expression of model genes between BC and normal tissue on the basis of Human Protein Atlas (HPA) database via immunohistochemistry (IHC).

2.9. Statistical analysis

All statistical analyses were performed using R (v.4.1.0), and *P-value* < 0.05 was considered as statistically significant. Comparison of continuous variables between groups was analyzed with the independent t-test. Moreover, chi-square test was performed to examine categorical data. The Wilcoxon test was applied to identify correlations between groups defined by IRGS score.

3. Results

3.1. Identification of differentially expressed IFN-γ related genes

On the basis of TCGA cohort, 93 differentially expressed IFN-γ related genes were identified using the differentially expressed gene analysis (Table S3; Fig. 1A, B). Next, we assessed the CNV in the differentially expressed IFN-γ related genes and witnessed extensive copy number alterations in above genes. Among them, 25 genes (*ARID5B, EIF4E3, IL10RA, NFKBIA, PDE4B, SOD2, TNFAIP6*, etc) possessed CNV decreases, while 67 genes (*APOL6, BPGM, CMPK2, CXCL10, CXCL11, CXCL9, DHX58*, etc) had CNV increases (Figure 1C). Figure 1D showed the locations of the CNV alterations in the differentially expressed IFN-γ related genes on their respective chromosomes. Refer to Table S3, we found a positive correlation between majority of genes expression levels

and CNV alteration. Differentially expressed IFN-γ related genes with CNV loss, such as *ARID5B, EIF4E3, IL10RA, NFKBIA, PDE4B, SOD2*, and *TNFAIP6*, were decreased in BC samples compared with normal bladder samples (logFC <0), while 45 genes with CNV gain, such as *APOL6, BPGM, CMPK2, CXCL10, CXCL11, CXCL9*, and *DHX58*, were increased in BC samples compared with normal bladder samples (logFC >0). These implied that CNV might be a regulatory factor of the mRNA expression of IFN-γ related genes.

As shown in Fig. S2A, a number of enriched gene sets were found using GO enrichment analysis. The biological process (BP) of the IFN-γ related differentially expressed genes were mainly enriched in response to virus, defense response to virus and defense response to symbiont. In the cellular component (CC) analysis, proteasome complex, endopeptidase complex and peptidase complex were considered to be relevant to the IFN-γ related differentially expressed genes. In addition, for the result of the molecular function (MF), it was suggested that these genes were mainly involved in cytokine receptor binding, ubiquitin−like protein ligase binding and endopeptidase activity. The top three enriched pathways for the KEGG pathway analysis were Influenza A, Herpes simplex virus 1 infection and Epstein−Barr virus infection (Fig. S2B). As shown in Fig. S2C, differentially expressed genes were screened into the PPI network complex via the STRING website.

3.2. Classifying of molecular subtypes

Based on these differentially expressed IFN-γ related genes, the NMF consensus clustering was carried out to classify the molecular subgroups. It was found that the two subgroups (C1, C2) had clear boundaries at K = 2 (Fig. 2A, B). After a comprehensive consideration, K of 2 as the optimal k-value was determined. Then, PCA was applied to verify the rationality of above subtypes. As displayed in Figure 2C, the there-dimensional PCA plot clearly describes a clear separation of different populations for each sample. Moreover, survival analysis using the K-M curve suggested that C1 subtype had a poorer OS than that in C2 subtype (Figure 2D).

To explore immune condition of the two subtypes, we conducted ESTIMATE and MCP-counter algorithms for the TCGA gene expression profile based on the subgroups. It was discovered that stromal score, immune score, and ESTIMATE score were upregulated in C1 subtype (Fig. 3A-C), while tumor purity were enriched in C2 subtype (Figure 3D). Meanwhile, MCP-counter algorithm indicated that significantly increased B cell lineage, CD8 T cells, cytotoxic lymphocytes, fibroblasts, monocytic lineage, and NK cells were observed in C1 subtype compared with C2 subtype (Fig. 3E-J), while the opposite was witnessed for neutrophils (Figure 3K). In view of the fact that the blockade of immune checkpoints has become a vital strategy in the treatment of BC. We then evaluated a slice of immune checkpoints expression levels between BC subtypes. The results demonstrated that the expression levels of *CD274(PD-L1), PDCD1 (PD-1), CTLA4, LAG3, TIGIT*, and *HAVCR2* were higher in C1 subtype than that in C2 subtype (Fig. 4A-F), revealing that C1 subtype was more amenable to the formation of tumor-immunosuppressive microenvironment, which subsequently drove tumor immune escape [43]. This also explained why C1 subtype had a poorer OS than that in C2 subtype. The above studies had suggested that molecular subtype based on differentially expressed IFN-γ related genes could distinguish the outcome of patients, and was associated with the components of the TIME and the expression levels of immune checkpoints.

Table 1. Clinical characteristics of the 4 bladder cancer patients.

| Patient number	Age (years)	Gender	Histologic grade	T classification	M classification	N classification	Surgical procedure
1	58	Male	High Grade	T1	M0	Unknow	Laparoscopic radical cystectomy
2	74	Female	High Grade	T3	M0	Unknow	Laparoscopic radical cystectomy
3	52	Male	High Grade	T2	M0	N0	Laparoscopic radical cystectomy
4	59	Male	High Grade	T1	M0	N0	Laparoscopic radical cystectomy
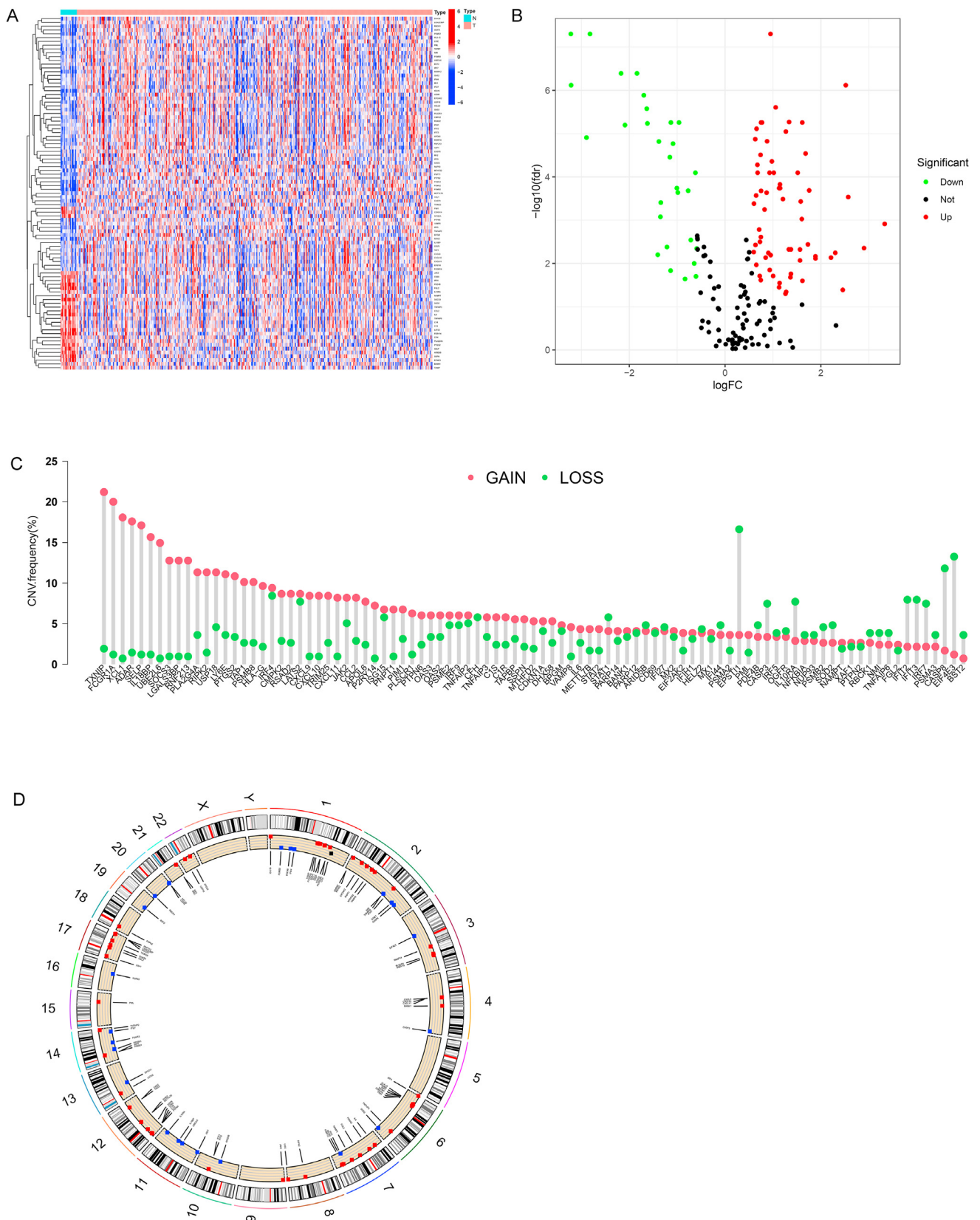
Figure 1. Genetic and transcriptional alterations of differentially expressed IFN-γ related genes in BC **(A)** Heatmap of differentially expressed genes between BC and normal tissues in the TCGA cohort **(B)** Volcano diagram of differentially expressed IFN-γ related genes based on TCGA database **(C)** Frequencies of CNV gain, loss, and non-CNV among differentially expressed IFN-γ related genes **(D)** Locations of CNV alterations in differentially expressed IFN-γ related genes on 23 chromosomes. IFN-γ, Interferon gamma; BC, bladder cancer; TCGA, The Cancer Genome Atlas; CNV, copy number variant.
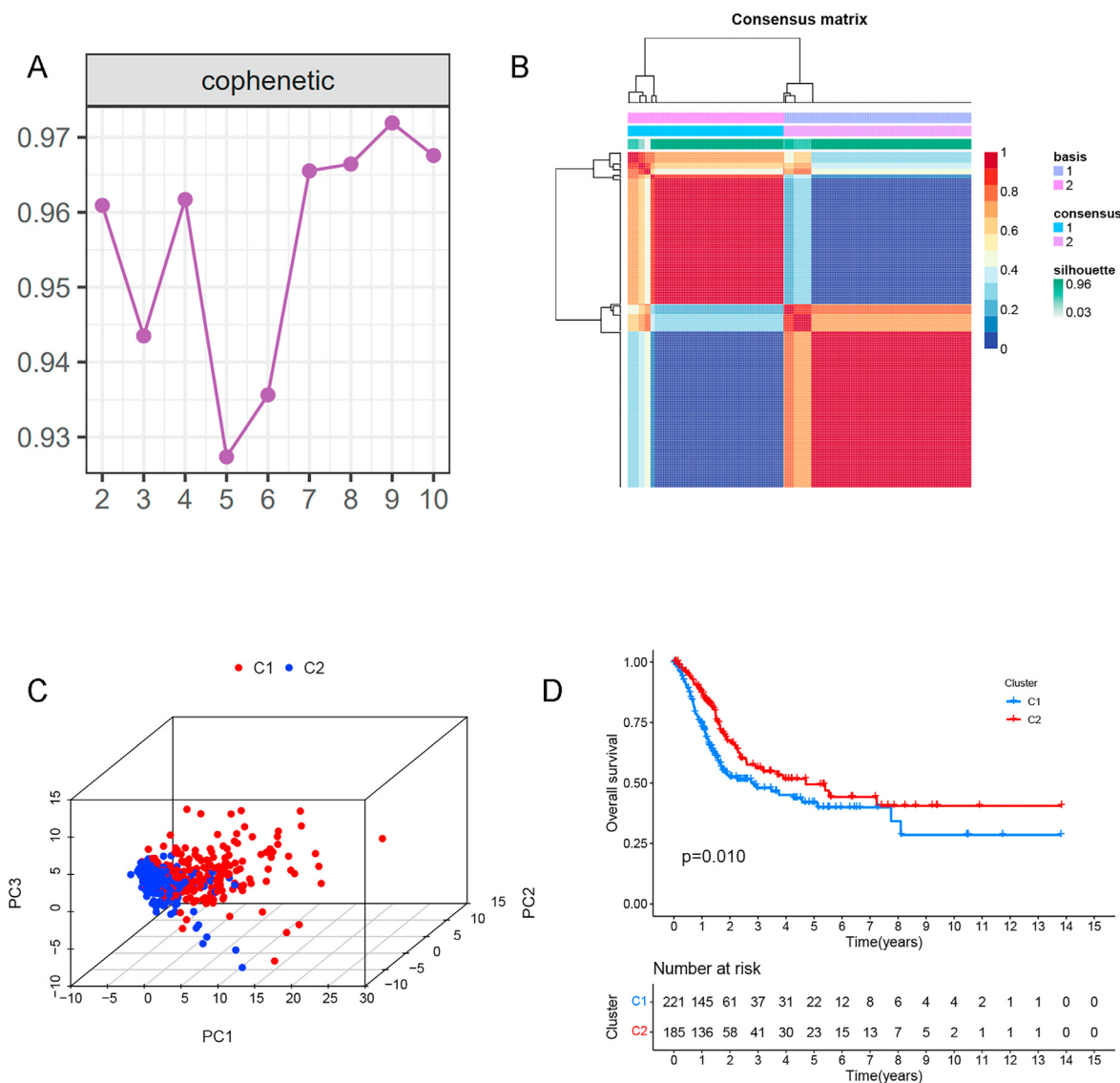
Figure 2. Identification of molecular subgroups through nonnegative matrix factorization (NMF) cluster **(A)** The cophenetic correlation coefficient for the cluster number from 2 to 10 **(B)** The two molecular subgroups were determined when k = 2 **(C)** Principal component analysis (PCA) for the BC patients **(D)** Survival analysis for the overall survival of the molecular subgroups in BC. BC, bladder cancer.

3.3. Construction and testing of prognostic signature

Given that the close correlation between differentially expressed IFN-γ related genes and outcome and immune profile of BC, we attempted to construct a model based on the IFN-γ related genes signature for their prognostic value and immunotherapeutic efficacy. Afterwards, 24 genes most associated with overall survival were further determined by univariate Cox regression analysis (Fig. S3). After above filtration, a stepwise multivariate Cox regression analysis was carried out to sort out eight prognostic IFN-γ related genes (*LATS2, MTHFD2, VAMP8, IRF5, RIPK2, HLA-G, APOL6* and *PTPN6*) and established a risk signature. The risk score of each patient was calculated using the following formula: risk score = expression value of *LATS2* * 0.4097 + expression value of *MTHFD2* * 0.2446 + expression value of *VAMP8* * 0.2262 - expression value of *IRF5* * 0.1809 - expression value of *RIPK2* * 0.2269 - expression value of *HLA-G* * 0.2476 - expression value of *APOL6* * 0.3725 - expression value of *PTPN6* * 0.3751.

Then, patients were grouped according to the median risk score of TCGA cohort: the high IRGS group (risk score > the median-risk score)

and the low IRGS group (risk score ≤ the median-risk score). TCGA and GEO cohorts patients survival statuses and selected genes expression profile were illustrated in Figures 5A and Fig. 5B. To explore the prediction ability of the IRGS on the outcome of BC patients, we also generated K-M and survival-ROC curves. The results of survival analysis suggested that high IRGS score group had a poorer OS (Fig. 5C, D) than that in low IRGS score group in TCGA and GEO cohorts.

Also, the patients of high-risk score group showed worse DFS, DSS, and PFS outcome (Fig. 5E-G) compared with those in low-risk score group based on risk score optimal cutoff in TCGA cohort. ROC curves indicated that 1-year AUC = 0.721, the 3-year AUC = 0.697 and the 5-year AUC = 0.709 of IRGS in TCGA cohort (Figure 6A), and 1-year AUC = 0.663, the 3-year AUC = 0.639 and the 5-year AUC = 0.638 of IRGS in GEO cohort (Figure 6B). We then conducted univariate and multivariate Cox regression analyses to confirm the independent prognostic value of our signature in OS prediction. The results proved the independent prognostic value of IRGS in TCGA cohort (Figure 6E). Then, it was found that there was a positive correlation between risk score levels and clinical features (age, histological grade, clinical stage, T
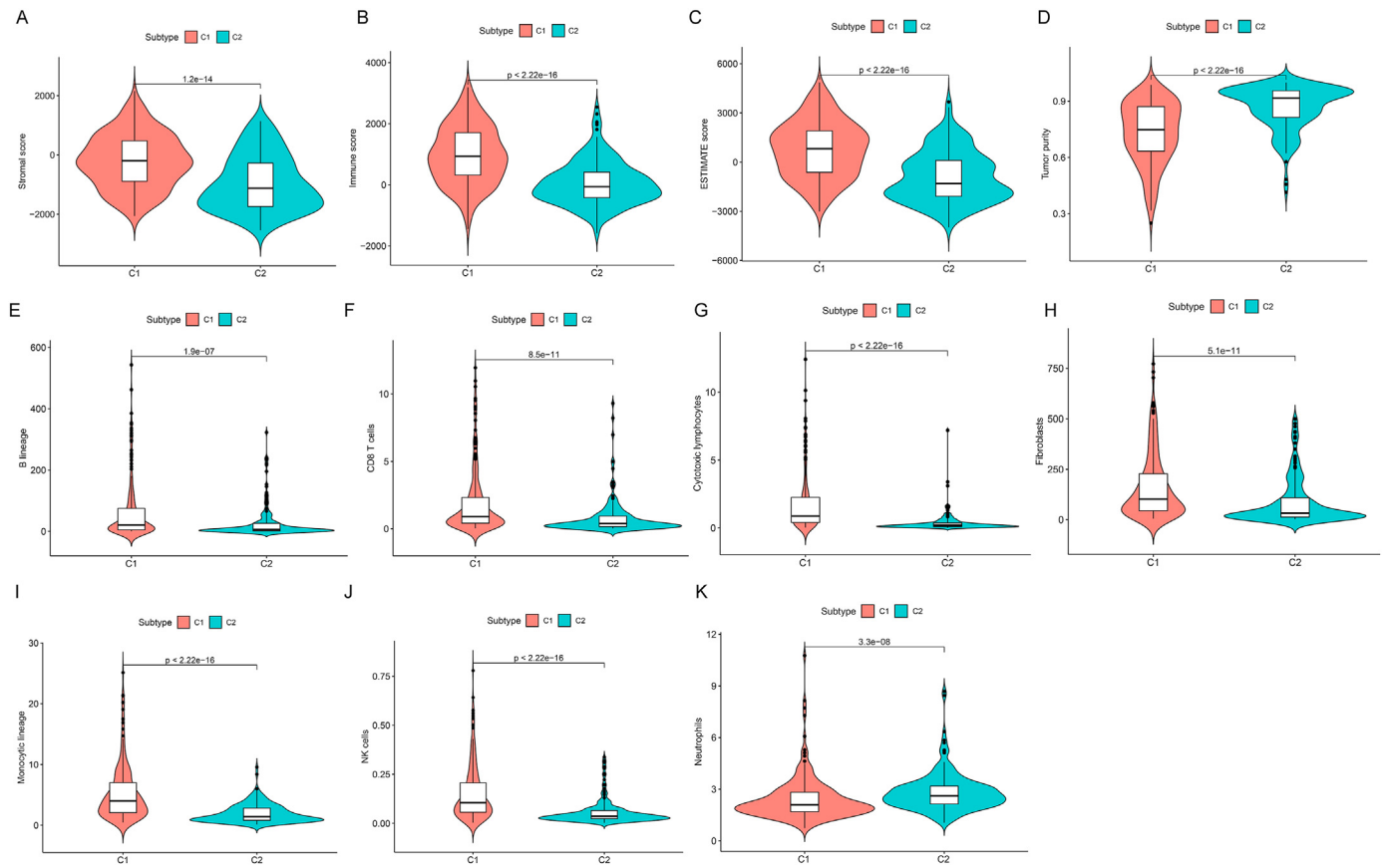
Figure 3. Immune profile of the two molecular subgroups. The comparisons of stromal score **(A)**, immune score **(B)**, ESTIMATE score **(C)**, and tumor purity **(D)** between the two subgroups. Infiltration levels of B cell lineage **(E)**, CD8 T cells **(F)**, cytotoxic lymphocytes **(G)**, fibroblasts **(H)**, monocytic lineage **(I)**, NK cells **(J)**, and neutrophils **(K)** that were calculated by the MCP-counter algorithm in the two subtypes. MCP-counter algorithm, the microenvironment cell-population counter algorithm.
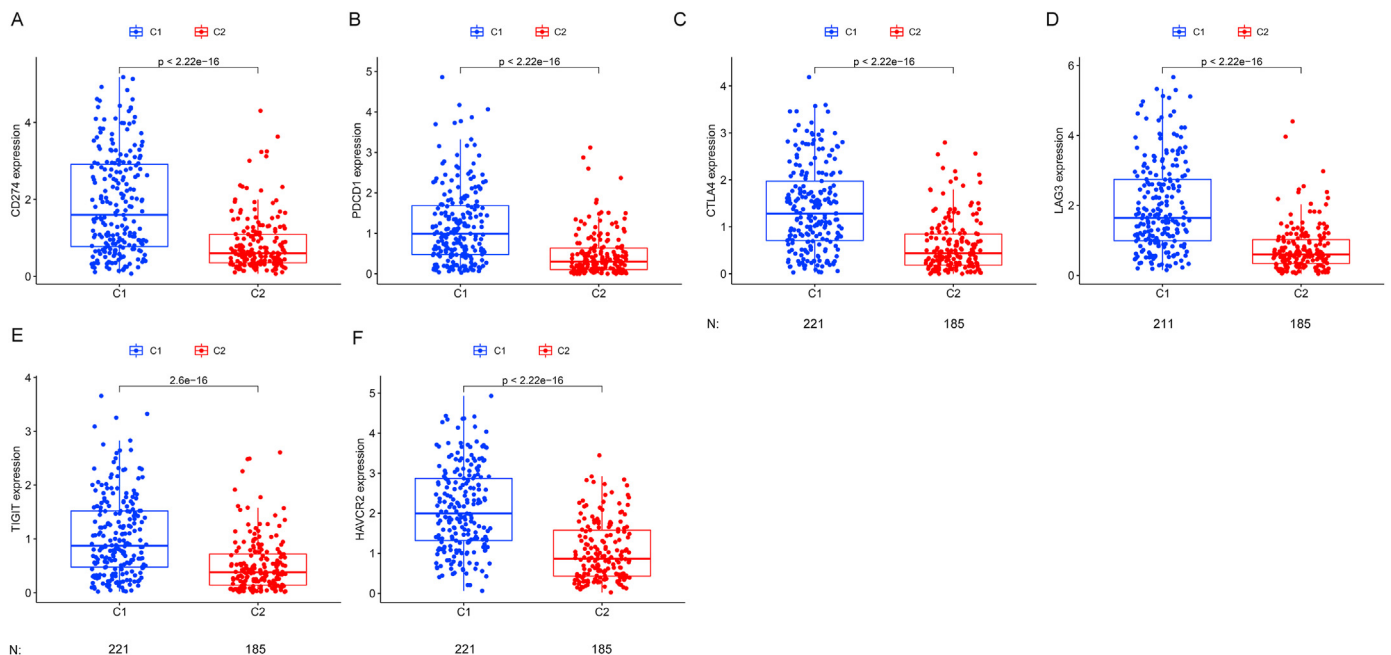
Figure 4. Immune checkpoint molecules expression levels of the two molecular subgroups. The expression levels of *CD274* **(A)**, *PDCD1* **(B)**, *CTLA4* **(C)**, *LAG3* **(D)**, *TIGIT* **(E)**, and *HAVCR2* **(F)** between the two subgroups. The number of patients with specific clinical information for each subtype is detailed below the bar plot (N).
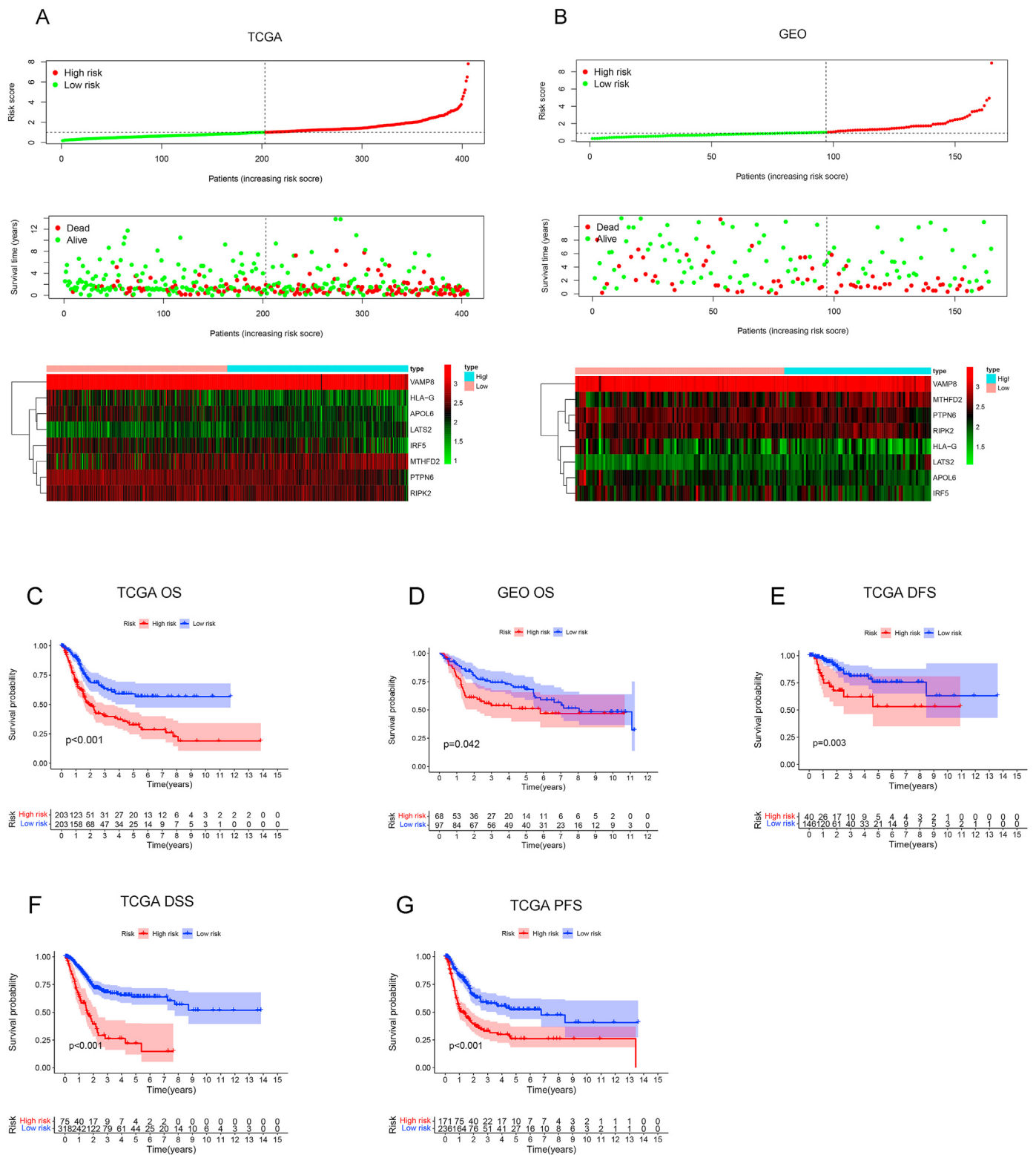
Figure 5. Evaluation of IRGS. BC patients' survival statuses and selected genes expression profile in TCGA **(A)** and GEO cohorts **(B)**. The patient risk curve defined by risk score. Scatter plot showing whether the patients were alive. Heatmap showing the expression levels of the eight IFN-γ related genes. K-M curves analyses suggested that high IRGS score group had a poorer OS than that in low IRGS score group in TCGA **(C)** and GEO cohorts **(D)**. High risk score group enjoyed poorer DFS **(E)**, DSS **(F)**, and PFS **(G)** than that in low score group based on risk score optimal cutoff in TCGA cohort. BC, bladder cancer; TCGA, The Cancer Genome Atlas; GEO, Gene Expression Omnibus; IRGS, the interferon-γ related gene signature; K-M, Kaplan-Meier; OS, overall survival; DFS, disease-free survival; DSS, disease-specific survival; PFS, progression-free survival.
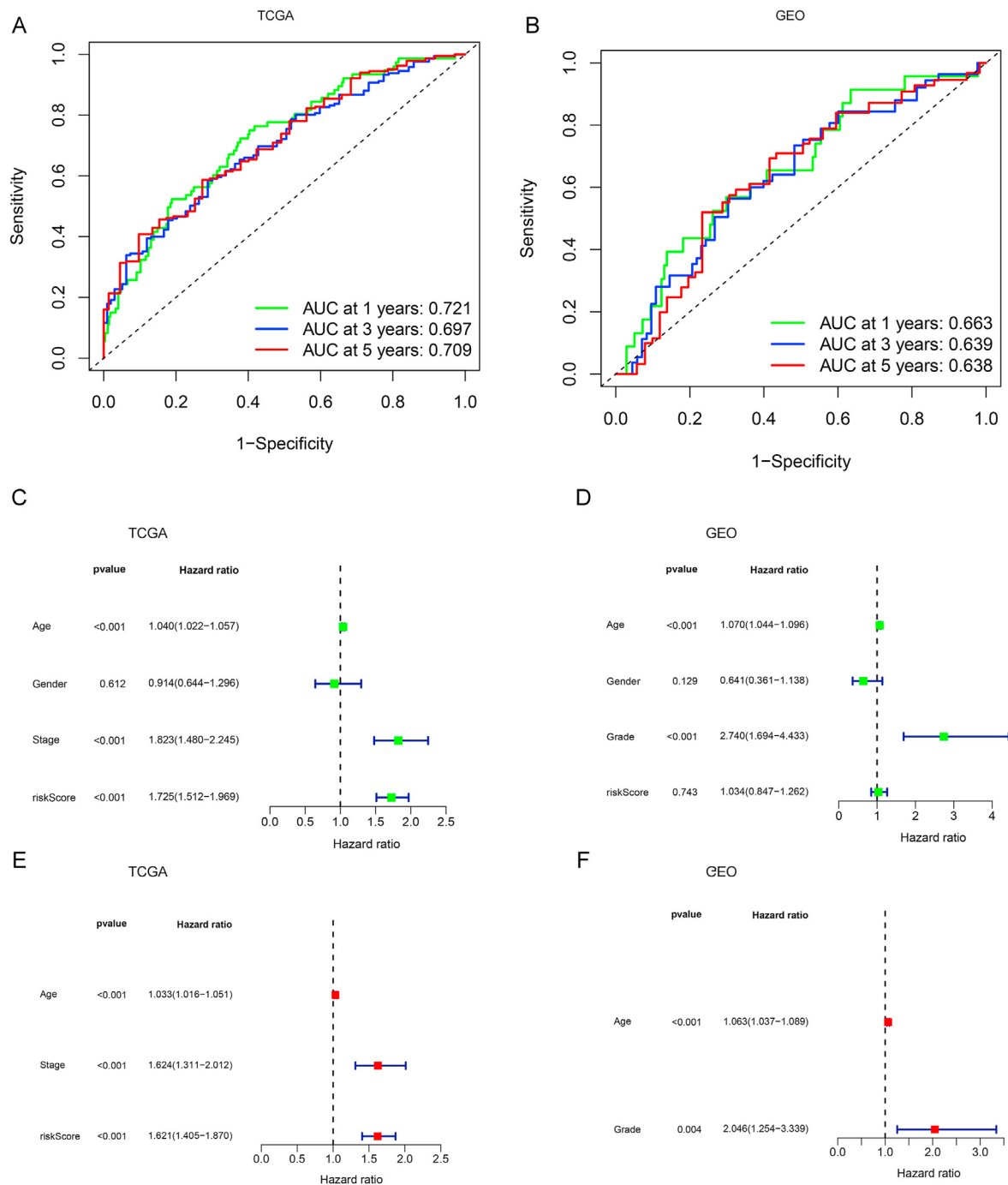
Figure 6. Testing of IRGS. ROC curves indicated that 1-year AUC = 0.721, the 3-year AUC = 0.697 and the 5-year AUC = 0.709 of IRGS in TCGA cohort **(A)**, and 1-year AUC = 0.663, the 3-year AUC = 0.639 and the 5-year AUC = 0.638 of IRGS in GEO cohort **(B)**. Univariate Cox analyses showed that IRGS was correlated with OS of BC patients in TCGA **(C)** cohort. Multivariate Cox analyses demonstrated IRGS was independently associated with OS of BC patients in TCGA **(E)** cohort. IRGS, the interferon-γ related gene signature; TCGA, The Cancer Genome Atlas; GEO, Gene Expression Omnibus; BC, bladder cancer; OS, overall survival; ROC, receiver operating characteristic; AUC, area under the curve.

classification, N classification, and M classification) (Fig. 7A, B). In summary, these results suggested that samples with higher risk score possessed a tendency for poor prognosis.

3.4. The prognostic nomogram

To apply the results of this study to clinical practice in a quantitative approach, the independent predictors (IRGS, age, and stage) were involved to construct a nomogram for the prediction of TCGA patients' OS probability of 1-year, 3-year and 5-year (Figure 8A). The calibration

curves of above nomogram proved preferable agreement between nomogram-predicted OS and actual OS (Figure 8B). The ROC curves and C-index implied that the diagnose ability of nomogram was more precise than those of clinical stage and IRGS alone, and the reliability of nomogram for predict OS was superior to IRGS alone (Fig. 8C-F).

3.5. Functional analyses of the high and low IRGS groups

To identify differentially activated signaling pathways in the high IRGS and low IRGS groups, GSEA based on the KEGG gene sets was
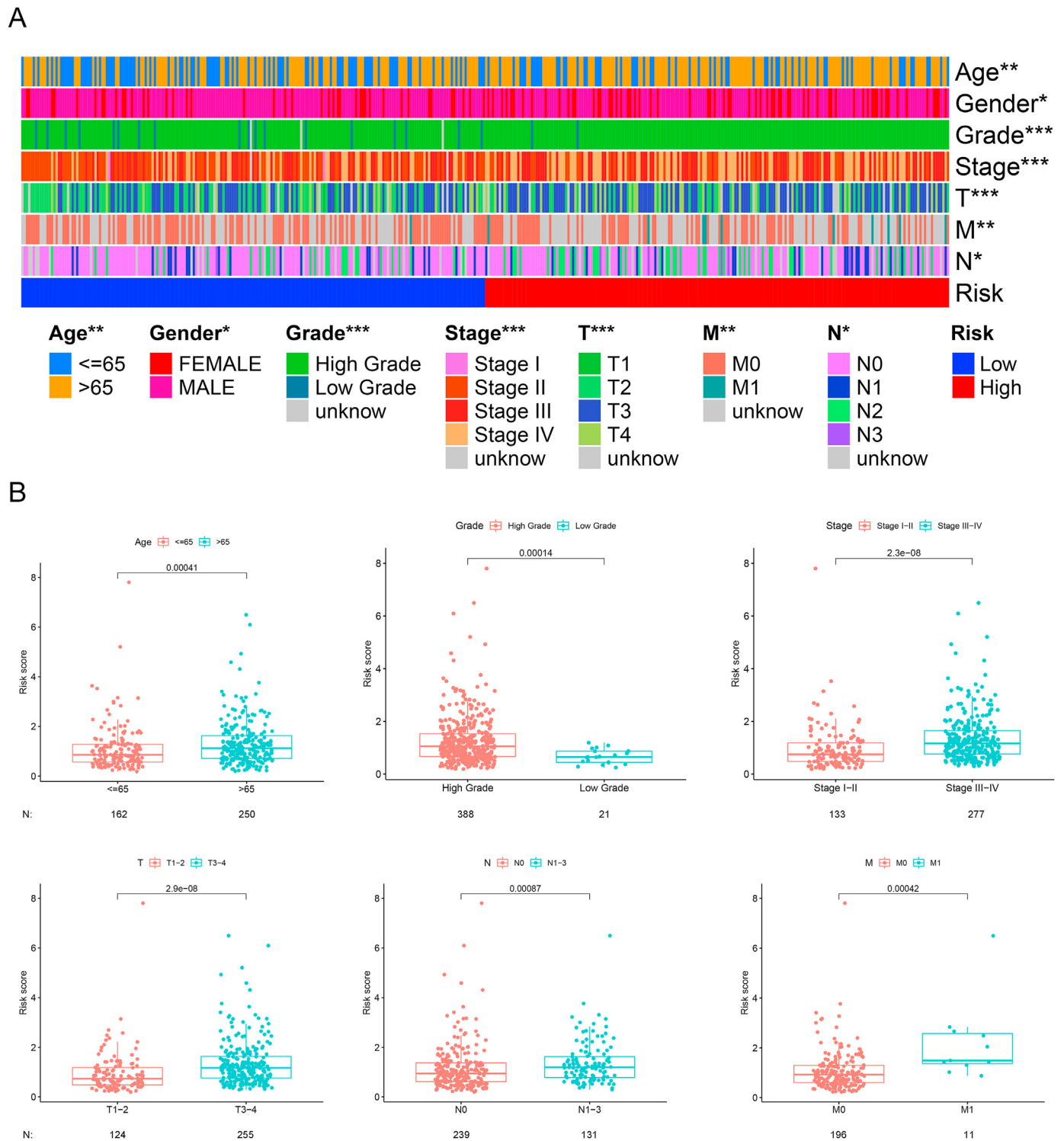
A

B

Figure 7. Relationships between IRGS and clinical features **(A)** The heatmap of relationships between IRGS and clinical features in the TCGA cohort **(B)** Relationships between IRGS and age, histological grade, pathological stage, T stage, N stage, and M stage. The number of patients with specific clinical information for each subtype is detailed below the bar plot (N); * represents *P value* < 0.05, ** represents *P value* < 0.01, and *** represents *P value* < 0.001; IRGS, the interferon-γ related gene signature; TCGA, The Cancer Genome Atlas.

conducted. It was found that the top five of most significantly related signaling pathways, including dilated cardiomyopathy, hypertrophic cardiomyopathy, melanoma, and two tumor-progression related pathways (focal adhesion, ECM-receptor interaction) [44, 45, 46], were enriched in the high IRGS group (Fig. S4A). Meanwhile, five pathways were enriched in the low IRGS group (Fig. S4B).

3.6. Immune and molecule characteristics of the two IRGS groups

To assess immune condition of the IRGS groups, we conducted ES-TIMATE algorithm for the TCGA gene expression profile based on the subgroups. It was found that stromal score was upregulated in the high IRGS group, while immune score was enriched in the low IRGS group
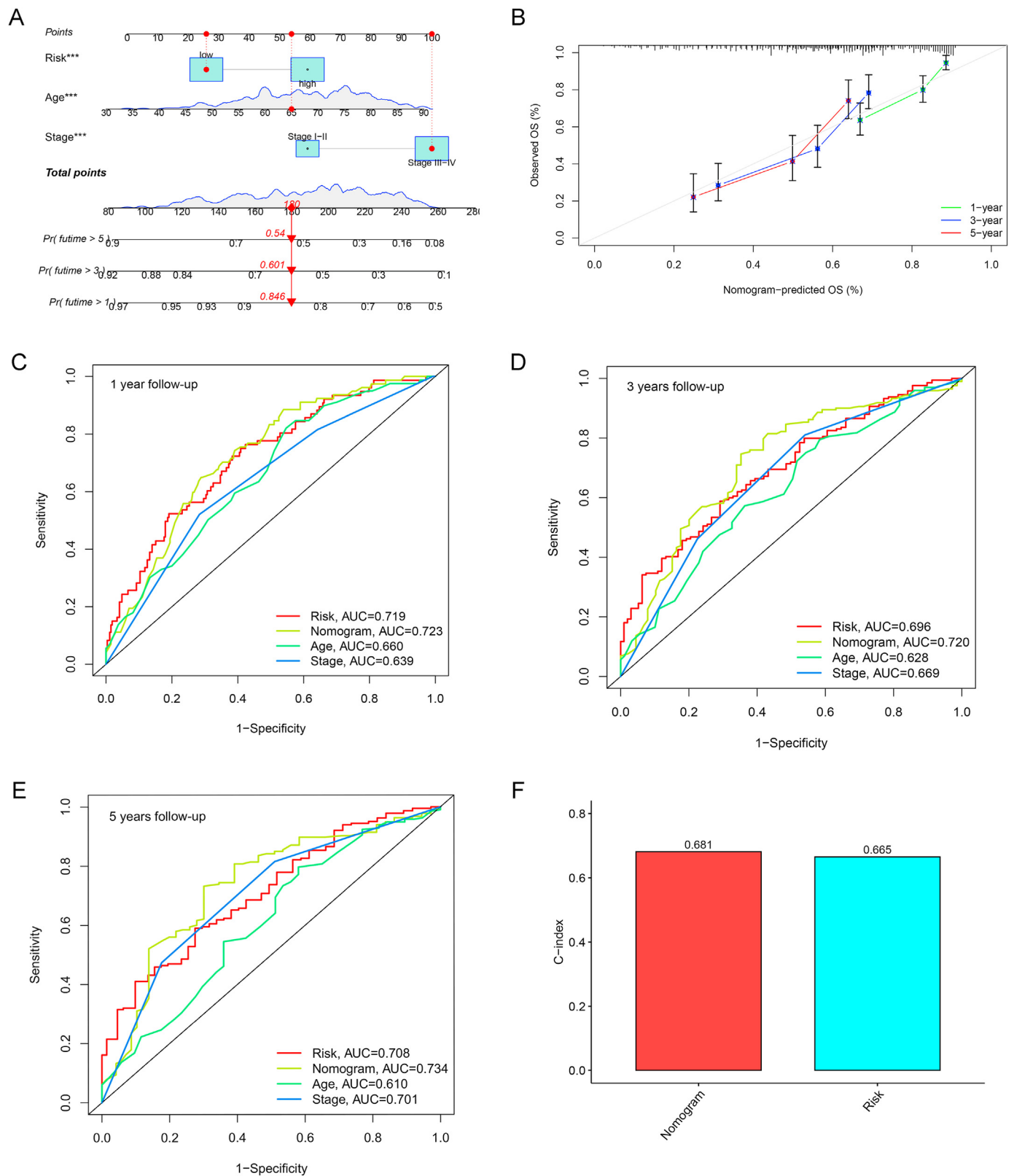
Figure 8. The prognostic nomogram **(A)** The nomogram for the prediction of BC patients' OS probability of 1-year, 3-year, and 5-year **(B)** The calibration curves of the nomogram showed good agreement between nomogram-predicted 1, 3, 5-years OS probability and actual 1, 3, 5-years OS probability. The ROC curves indicated that the diagnose ability of IRGS was more precise than those of clinical stage and IRGS alone at 1 **(C)**, 3 **(D)**, and 5 **(E)** years follow-up **(F)** C-index of the nomogram was 0.681, which was obviously higher than those of the IRGS. *** represents *P value* < 0.001. BC, bladder cancer; OS, overall survival; ROC, receiver operating characteristic; C-index, concordance index; IRGS, the interferon-γ related gene signature.
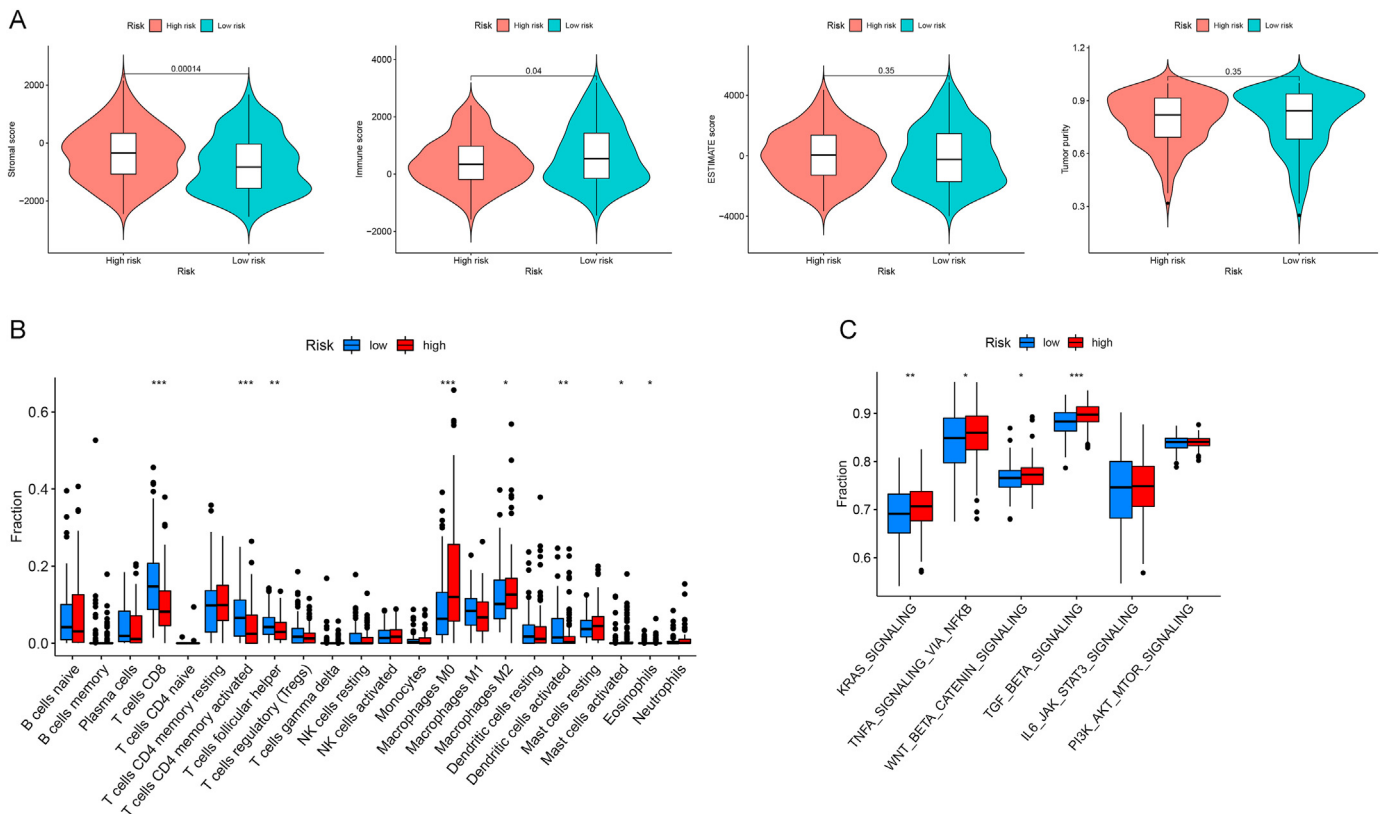
Figure 9. Immune and molecule characteristics of the two IRGS groups **(A)** The comparisons of stromal score, immune score, ESTIMATE score, and tumor purity between the two subgroups **(B)** The difference of immune cells infiltration levels between the two IRGS groups **(C)** The different distribution of pro-oncogenic signals between the two IRGS groups. * represents *P value* < 0.05, ** represents *P value* < 0.01, and *** represents *P value* < 0.001; IRGS, the interferon-γ related gene signature.
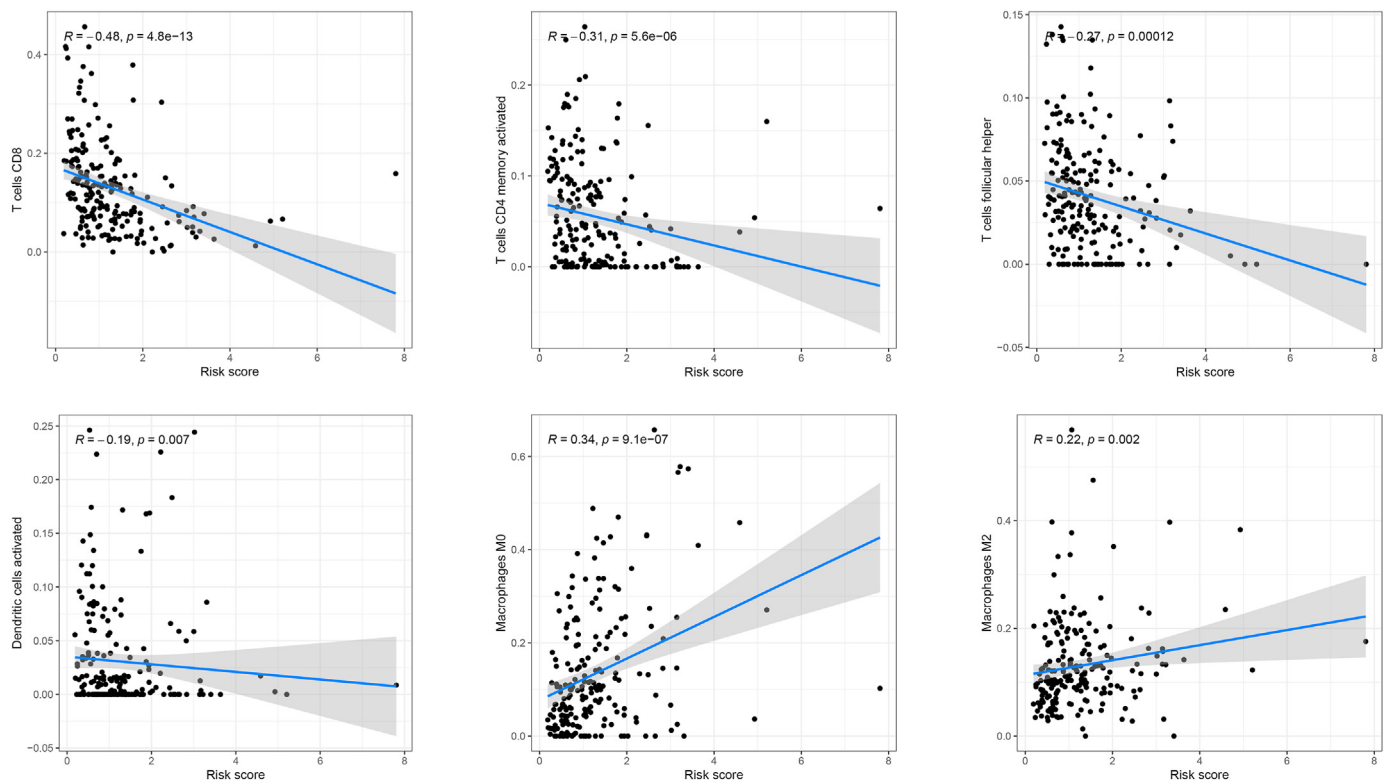

Figure 10. The correlation between IRGS and the immune infiltrating cells. IRGS, the interferon-γ related gene signature.

(Figure 9A). Further, to probe the relevance between IRGS and the immunocyte infiltration, the profile of immunocytes were estimated in the two IRGS groups through CIBERSORT algorithm. The results inferred that Macrophages M0 and Macrophages M2 predominate in the high IRGS group, while the opposite was witnessed for T cells CD8, T cells CD4 memory activate, T cells follicular helper and Dendritic cells activated (Figure 9B). Meanwhile, the proportion of 22 kinds of immunocytes infiltrated in IRGS subgroups was also confirmed (Fig. S5). Afterwards, correlation analysis of risk score and immunocyte infiltration showed a consistency with those of difference analysis (Figure 10). In addition, hallmark gene set was carried out to define the molecular function between different IRGS groups. As shown in Figure 9C, GSVA results suggested that tumor-progression related pathways (KRAS, TNFa/NF-kB, WNT/β-catenin and TGF-β pathways) enriched in the high IRGS group.

Furthermore, we examined whether the prognostic value of IRGS came from better immunosuppression or more malignant tumor growth. For OS, it was found that samples with higher levels of M2 Macrophages, WNT/β-catenin, TGF-β, KRAS and TNFa/NF-kB pathways had a significantly worse outcome, while samples with higher level of CD8 T cells presented a favorable prognosis (Fig. S6). Consequently, above results implied that the prognostic value of IRGS might derive from stronger immunosuppression or more malignant tumor growth.

3.7. Relationship of IRGS with TMB and CSC index

Accumulating evidence proved that the high TMB was associated with improved response to ICI therapy [47]. Correlation analysis suggested that IRGS score was negative correlated with the TMB (Figure 11A). The top ten mutated genes in the two subgroups were TP53, TTN, KMT2D, MUC16, ARID1A, KDM6A, PIK3CA, SYNE1, RYR2, and KMT2C. The high IRGS group showed significantly higher

frequencies of TP53 and KMT2D mutations compared to those in the low IRGS group, while the opposite was witnessed for TTN and MUC16 (Fig. 11B, C). Also, tumor progression was known to be related to the stemness of cancer cells [48]. It was found that IRGS score was positive correlated with the cancer stem cell (CSC) index and the high IRGS group had the higher CSC index than that of the low IRGS group (Fig. 11D, E).

3.8. IRGS clustering is strongly linked to reported immune subtypes

Based on the genomic profiles of 33 non-hematologic TCGA cancer types, a solid tumors immune subtype has defined the immune landscape of malignancy as 6 immune subtypes: the wound healing (C1), the IFN-γ dominant (C2), the inflammatory (C3), the lymphocyte depleted (C4), the immunologically quiet (C5), and the TGF-βdominant (C6) [38]. As for BC, we try to explore the landscape of the reported immune subtype in the IRGS subgroups. In this paper, the low IRGS group comprised 30% C1 samples, 49% C2 samples, 6% C3 samples, and 15% C4 samples, while the high IRGS group comprised 59% C1 samples, 33% C2 samples, 5% C3 samples, and 3% C4 samples (Figure 12A). These results concluded that IRGS clustering was strongly linked to reported solid tumors immune classification ($p = 0.001$, chi-square test). Furthermore, we examined the connectedness between IRGS clustering and above molecular subgroups (C1, C2), and also found that the two were significantly associated (Figure 12B).

3.9. Analysis of immunotherapeutic response between IRGS subgroups

Subgroups immune checkpoints expression levels differed significantly as shown in Figure 13A, the expression levels of CD274(PD-L1), PDCD1 (PD-1), CTLA4, LAG3, and TIGIT in the low IRGS group were higher than that in the high IRGS group. Further, correlation analysis of
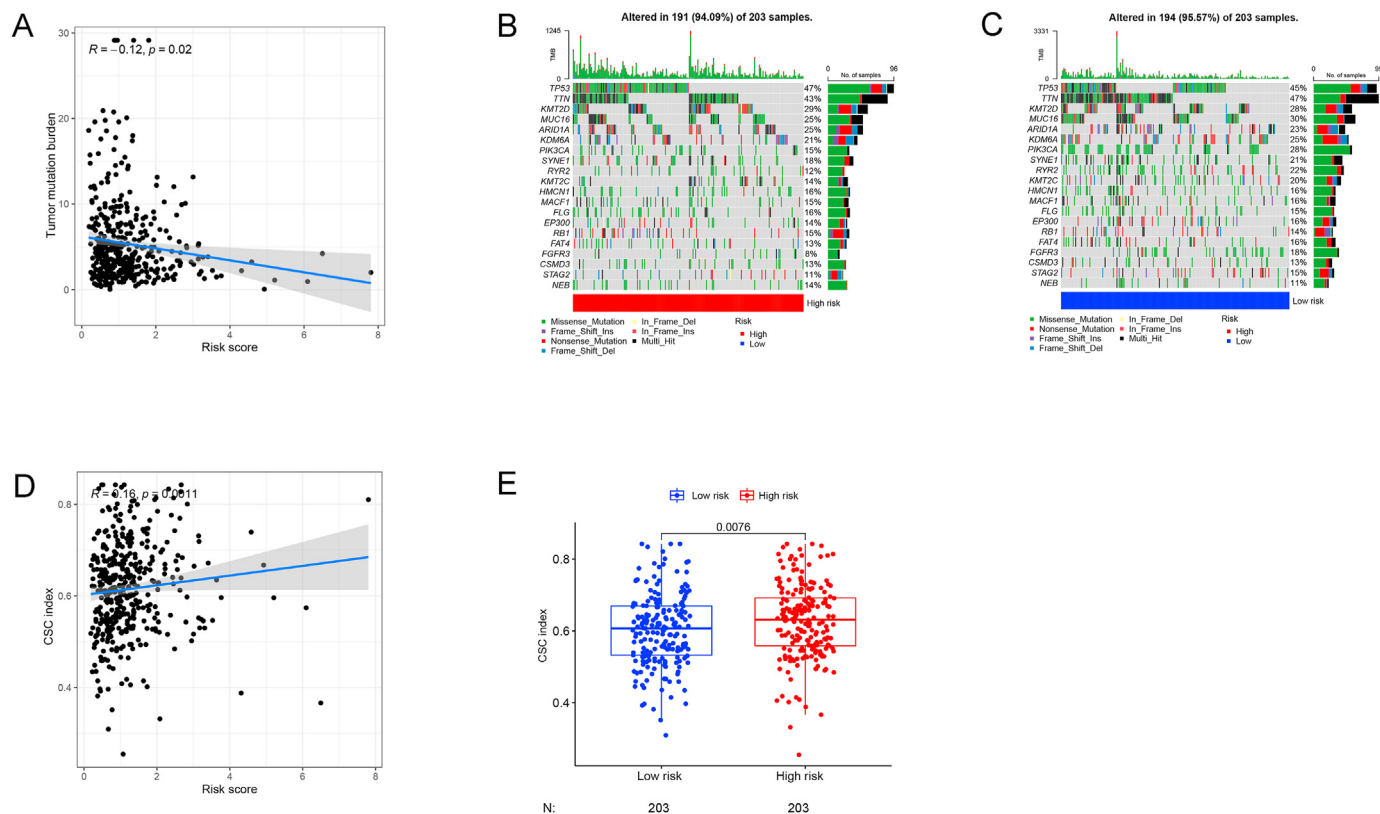

Figure 11. Relationship of IRGS with TMB and CSC index **(A)** IRGS score was negative correlated with the TMB **(B)** Mutated genes in the high IRGS subgroups **(C)** Mutated genes in the low IRGS subgroups **(D)** IRGS score was positive correlated with the CSC index **(E)** The high IRGS group had the higher CSC index than that of the low IRGS group. The number of patients with specific clinical information for each subgroup is detailed below the bar plot (N); IRGS, the interferon-γ related gene signature; TMB, tumor mutation burden; CSC, cancer stem cell.
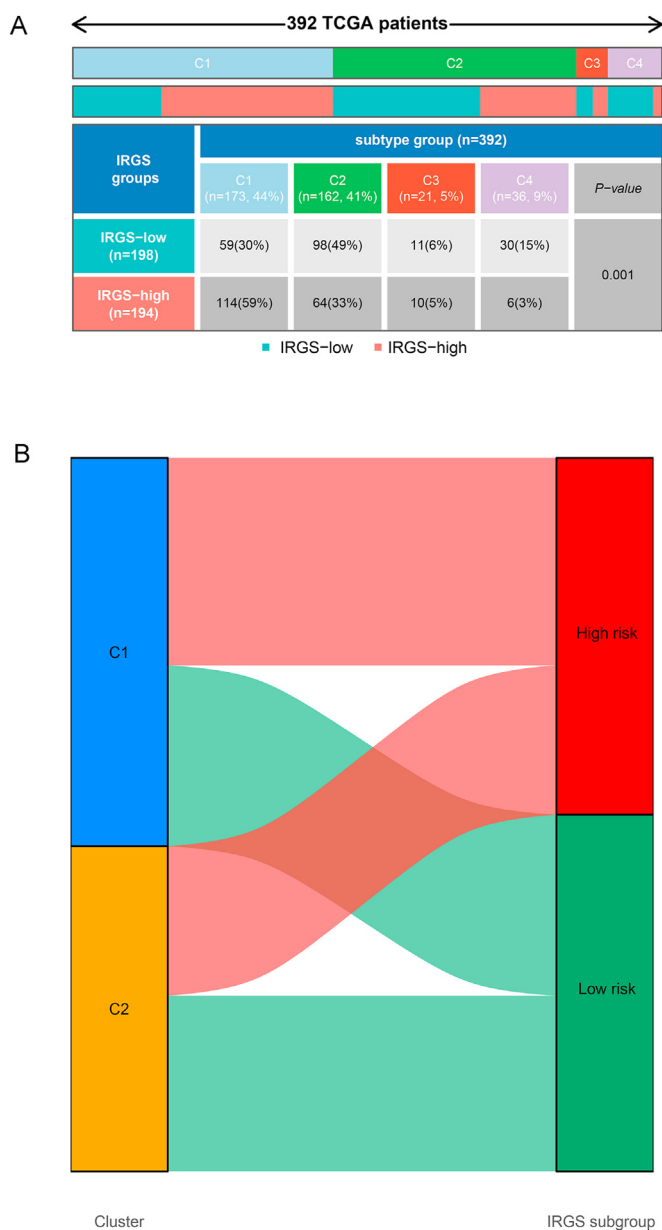
A

B

Figure 12. Relationship between the IRGS clustering and other classification **(A)** The IRGS clustering was related to the reported solid tumors immune classification **(B)** The connectedness between IRGS clustering and above molecular subgroups (C1, C2). IRGS, the interferon-γ related gene signature; TCGA, The Cancer Genome Atlas.

risk score and expression levels of immune checkpoints showed a consistency with above analysis (Figure 13B). It has previously been reported that BC patients with higher immune checkpoint expression gained more benefit of ICI compared to BC patients with low immune checkpoint expression [49]. Therefore, we speculated that the low IRGS group was more likely to benefit from ICI therapy.

To validate this conjecture, the relationship between immunophenoscore (IPS) obtained from TCIA and IRGS was probed in BC patients. IPS was supposed to predict the clinical response to immunotherapy in many tumors [50, 51]. Further analysis of the data revealed that the low IRGS group had the higher scores of IPS, IPS-CTLA4 blocker, IPS-PD1 blocker, and IPS-CTLA4 + PD1 blocker than the high IRGS group (Figure 14A), indicating that, compared to the high IRGS group, the low IRGS group might benefit more from the immunotherapy. To verify this finding, we further examined whether IRGS conferred prediction ability

of response to immunotherapy and prognosis in urothelial cancer patients with anti-PD-L1 therapy (IMvigor210 cohort). In our results, the high IRGS group also had a poorer OS than that in the low IRGS group (Figure 14B). Moreover, CR/PR (complete response/partial response) group had a lower IRGS scores compared with SD/PD (stable disease/progressive disease) group (Figure 14C). Then, we further attempted to explore different ICI benefits of two subgroups, and it was observed that patients in the low IRGS group had a higher CR/PR rate than those in the high IRGS group (Figure 14D). Based on above results of which corroborated each other, it is reasonable to believe that patients in the low IRGS group may be more sensitive to ICI therapy and development of precision ICI therapy strategy might benefit from employing IRGS in BC.

3.10. Potential drug sensitivity prediction

Besides ICI sensitivity therapy, we also investigated the IC_{50} differences of commonly used drugs in BC chemotherapy between IRGS subgroups. The lower IC_{50} value, the stronger the inhibitory effect of the drug on tumor growth. Then, we found that for methotrexate the low IRGS group were more sensitive than the high IRGS group (Figure 15A), while the opposite was witnessed for cisplatin (Figure 15B). These findings may exhibit implications for guiding the chemotherapy administration in BC.

3.11. RT-qPCR and IHC

To validate the potential role of the eight model genes (*LATS2, MTHFD2, VAMP8, IRF5, RIPK2, HLA-G, APOL6* and *PTPN6*) in BC progression, we further measured the eight genes expression levels with RT-qPCR. Compared with adjacent noncancerous tissues, *IRF5, LATS2, MTHFD2, VAMP8* and *PTPN6* expression levels were found to be broadly enhanced in paired BC tissues, and a reverse trend was observed in *HLA-G* (Figure 16A). However, the expression of the *RIPK2* and *APOL6* displayed no significant difference between tumor and the matched normal tissues (Fig. S7). As shown in Figure 16B, compared to the levels of protein in the normal bladder tissues, IRF5, MTHFD2, VAMP8 and PTPN6 were highly expressed in BC.

3.12. Comparison of models

Recently, we noticed that a number of predictive models effectiveness for predicting patients response to immunotherapy, such as TIDE and TIS signatures, have already been demonstrated. TIDE signature based on identifying the mechanisms of tumor immune escape and TIS signature constructed by quantitative and qualitative data of the TME had been demonstrated to be the valuable biomarkers in predicting response to ICI therapy [41, 42]. However, these two markers may place a higher importance on response to ICI while ignoring the patients clinical outcome, and lifespan is also critical for clinical decision. In this research, we compared the prognostic ability of the IRGS with the TIDE and TIS model using ROC curves and C-index in BC. It was found that the AUCs for IRGS were better than in that TIDE and TIS model at 1, 3, and 5 years follow-up (Fig. 17A-C). Similarly, these results also suggested that the c-index of the IRGS was 0.664, which was obviously higher than those of the TIDE and TIS (Figure 17D). These findings implied that the prognostic ability of IRGS is better than that of TIDE and TIS in BC.

4. Discussion

As a highly heterogeneous tumor, bladder cancer (BC) is the 9th leading cause of cancer-related deaths and the most prevalent malignancy of the urinary system [1]. Worldwide, the morbidity and mortality rate of BC remain elevated [52]. Surgical excision is the primary clinical treatment option for BC, however, about 70% of non-muscle invasive bladder cancer (NMIBC) patients suffer postoperative recurrence, while
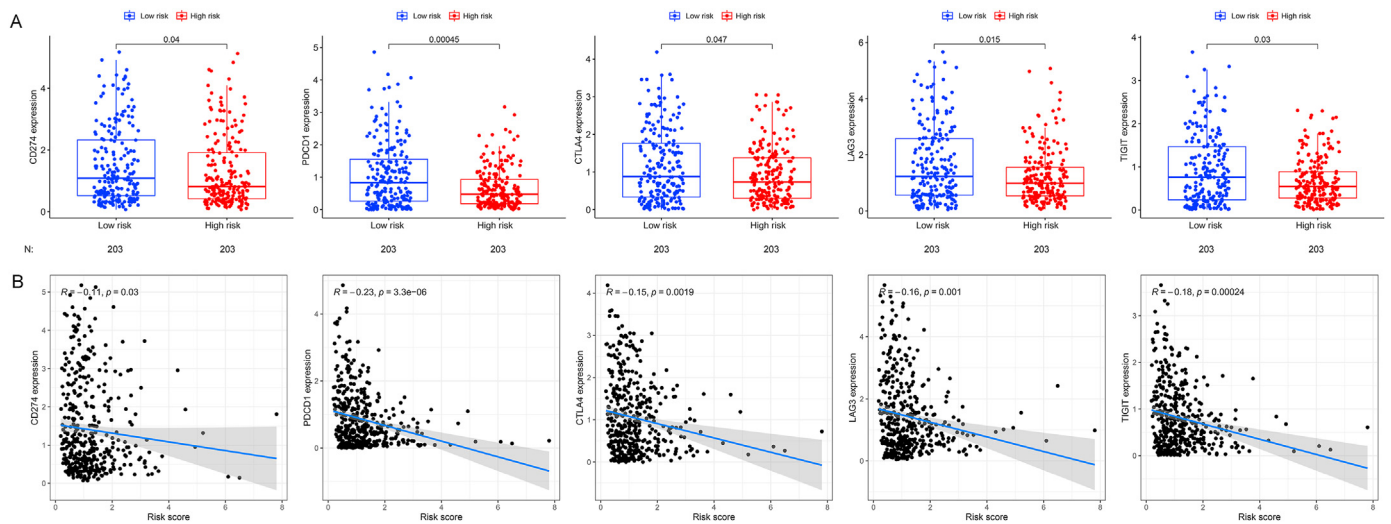
Figure 13. Immune checkpoint molecules expression levels of the IRGS subgroups **(A)** The expression levels of *CD274*, *PDCD1*, *CTLA4*, *LAG3* and *TIGIT* between the IRGS subgroups **(B)** The correlation between IRGS and the expression levels of the immune checkpoint molecules. IRGS, the interferon-γ related gene signature; The number of patients with specific clinical information for each subgroup is detailed below the bar plot (N).
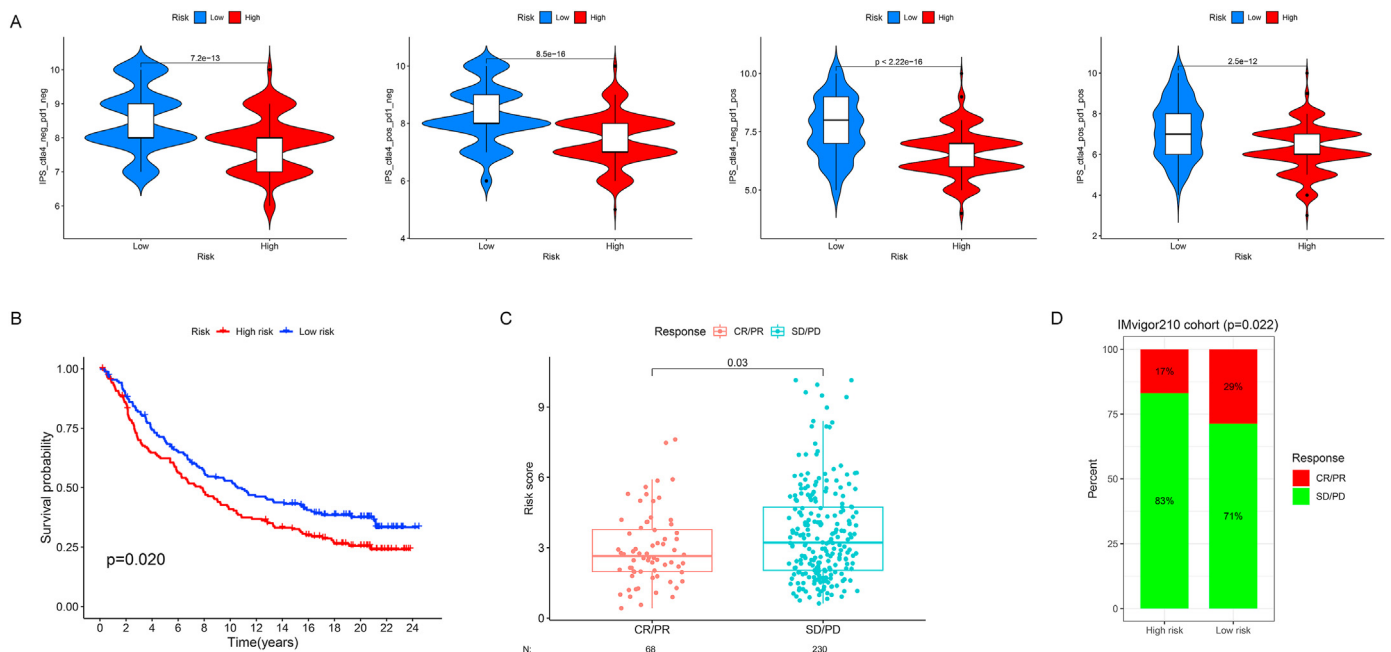

Figure 14. Analysis of immunotherapeutic response between the IRGS subgroups **(A)** The low IRGS group had a higher the scores of IPS, IPS-CTLA4 blocker, IPS-PD1 blocker, and IPS-CTLA4 + PD1 blocker than the high IRGS group **(B)** Survival analysis of the IRGS subgroups in IMvigor210 cohort **(C)** Distribution of IRGS score in groups with different anti-PD-L1 clinical response statuses **(D)** Rate of clinical response (CR/PR and SD/PD) to immunotherapy in two IRGS subgroups. The number of patients with specific clinical information for each subgroup is detailed below the bar plot (N); IRGS, the interferon-γ related gene signature; IPS, immunophenoscore; CR, complete response; PR, partial response; SD, stable disease; PD, progressive disease.

22–47% of muscle invasive bladder cancer (MIBC) patients recurred after standard radical surgery [53, 54]. For advanced bladder cancer, traditional therapies of BC including radiotherapy and chemotherapy incapable of controlling tumor progression effectively [10, 11, 12]. In recent years, the research fields of tumor immunity, the cancer metabolism and the TME continue to evolve rapidly. Especially in the field of tumor immunity, the discovery of tumor immune escape mechanism mediated by immune checkpoint molecules represented by PD-L1/PD-1 has opened a new era of BC immunotherapy [13]. However, only a limited proportion of BC patients experience clinical benefit due to the clinical response rates are far from sufficient [16]. To address this point, previous studies demonstrated that infiltrating regulatory T cells-induced suppressive tumor microenvironment is a critical obstacle for effective tumor immunotherapy [19]. Some reports pointed out that abundance of CD8 T cells infiltrated and PD-L1 expression levels in the TME could influence interindividual differences in immune checkpoint inhibitors response [20, 21, 22]. Zhang et al. found that the expression levels of *WDR5* were positively related to PD-L1, and the *WDR5* inhibitor could reduce PD-L1 expression induced by IFN-γ in BC [55]. Moreover, it was reported that activation of interferon stimulated genes was closely related to both superior prognosis and inferior prognosis following ICI therapy [32]. Consequently, a full and in-depth understanding of the relationship
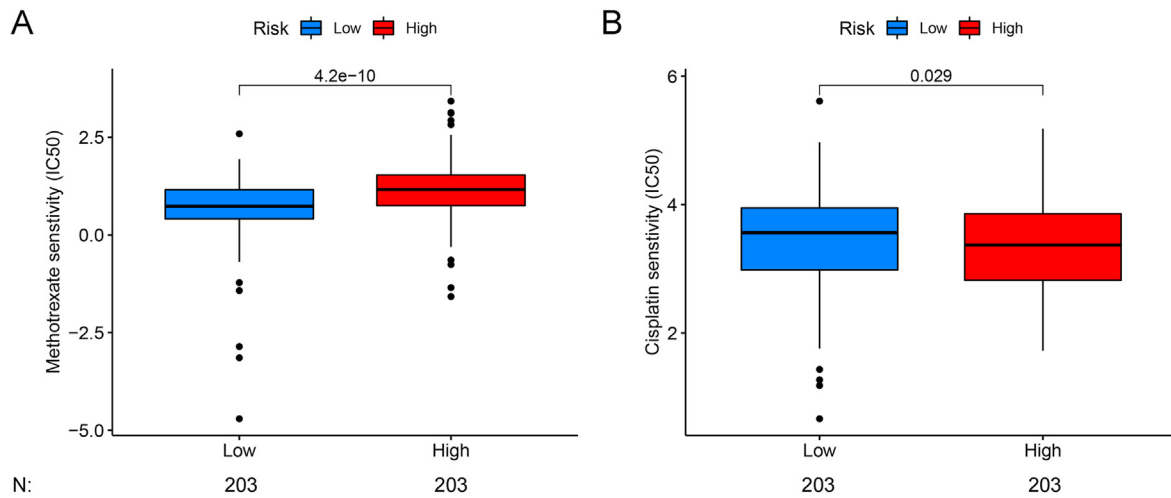
Figure 15. Differences of potential drug sensitivity in the IRGS subgroups. IC$_{50}$, half maximal inhibitory concentration; IRGS, the interferon-γ related gene signature. The number of patients with specific clinical information for each subgroup is detailed below the bar plot (N).
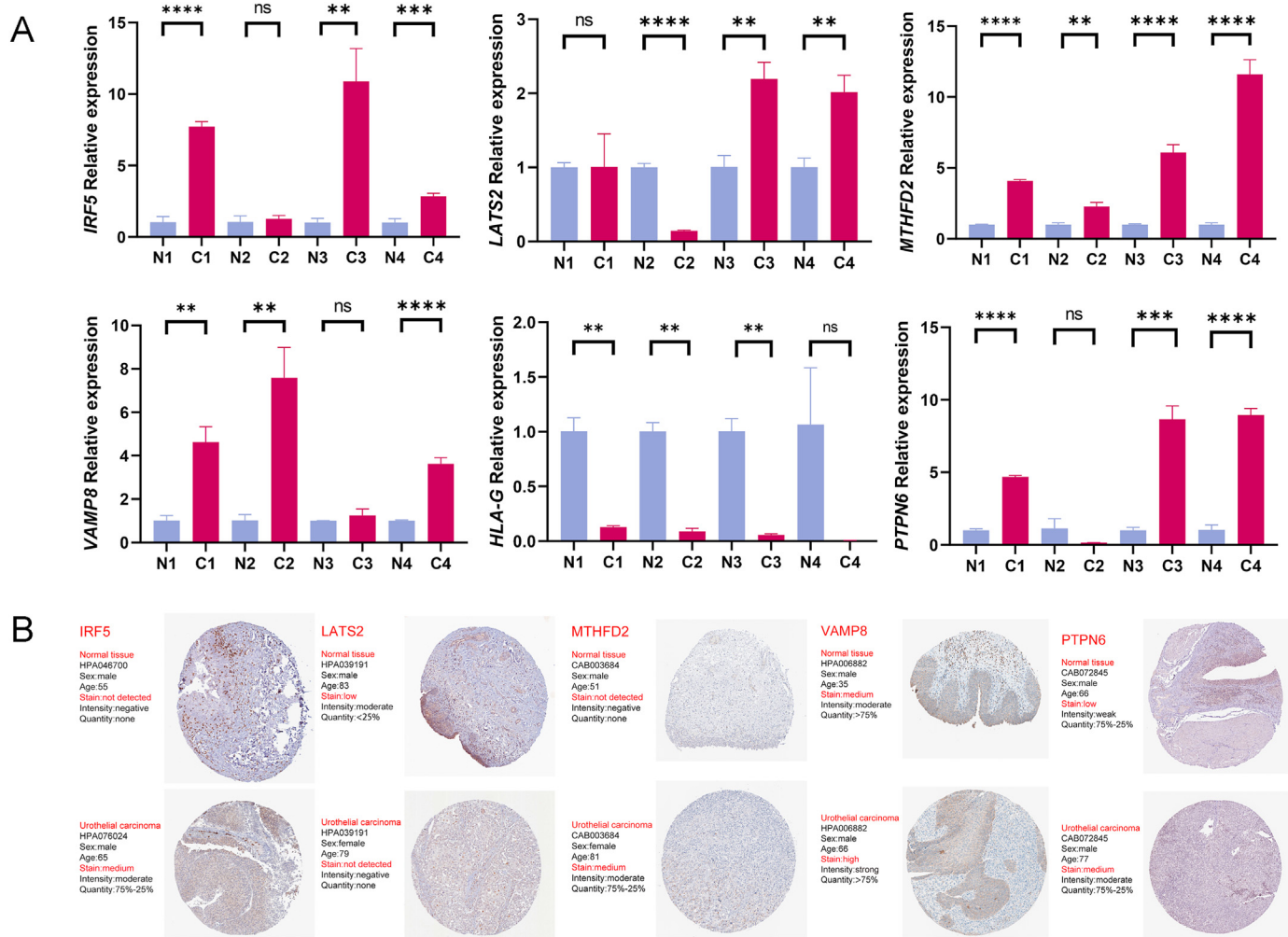

Figure 16. Validation of model genes expression levels **(A)** *IRF5, LATS2, MTHFD2, VAMP8, HLA-G* and *PTPN6* expression levels in four paired BC tissues (C1, C2, C3, C4) and adjacent noncancerous tissues (N1, N2, N3, N4) **(B)** Protein expression map of IRF5, LATS2, MTHFD2, VAMP8 and PTPN6 in the HPA database. Eight tissue samples (C1, N1, C2, N2, C3, N3, C4, N4) were used for RT-qPCR analysis; ns represents not significant, * represents *P value* < 0.05, ** represents *P value* < 0.01, and *** represents *P value* < 0.001; HPA database, Human Protein Atlas database; BC, bladder cancer.
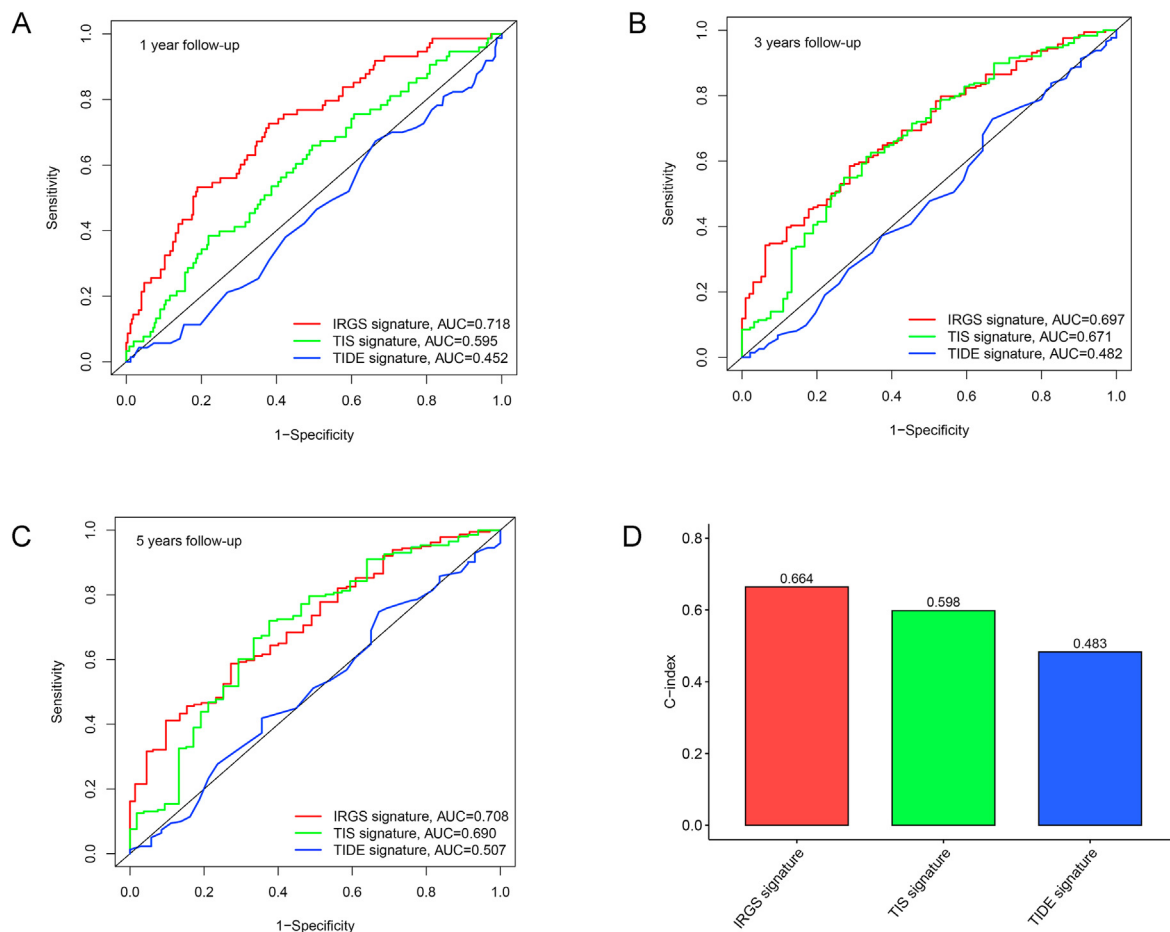
Figure 17. Comparison of models. AUCs for IRGS were better than in that TIDE and TIS model at 1**(A)**, 3 **(B)**, and 5 **(C)** years follow-up **(D)** C-index of the IRGS was 0.664, which was obviously higher than those of the TIDE and TIS. AUC, area under curve; IRGS, the interferon-γ related gene signature; TIDE, tumor immune dysfunction and exclusion; TIS, tumor inflammation signature; C-index, concordance index.

between the effectiveness of ICI therapy and infiltrating immunocytes in the TME and IFN-γ related genes might facilitate the awareness of the complex mechanism of BC resistance to immunotherapy.

Recent studies had suggested that molecular-based tumor typing can complement the pathological classification of tumors in clinical prognosis. The molecular biomarkers could provide more accurate clinical information for the diagnosis, treatment, and prognosis of patients [56, 57]. In addition, some studies suggested that the combination of molecular typing and pathological typing of tumors is superior to pathological typing alone in guiding clinical diagnosis and treatment. In this study, we presented a model associated with the TIME based on the filtered IFN-γ related genes that appeared to be helpful in BC risk stratification and prediction of immunotherapy responses. This can be clearly illustrated with the following analysis. First, molecular subtypes (C1 and C2 subgroups) based on differentially expressed IFN-γ related genes profile were determined using NMF clustering. Then, it can be noticed that significant differences existed in the OS, immune condition, and expression levels of major immune checkpoint molecules in the two subgroups. These indicated a certain link between differentially expressed IFN-γ related genes and both outcome and the TIME of BC. Second, we screened out eight IFN-γ related genes (*LATS2, MTHFD2, VAMP8, IRF5, RIPK2, HLA-G, APOL6* and *PTPN6*) associated OS of patients and established the IRGS based on above genes using univariate and multivariate Cox regression analyses. Afterwards, it was found that the IRGS could effectively distinguish the outcome of BC patients and have independent prognostic value. Third, we also witnessed that there were apparent discrepancies in immune profile and molecular characteristics between the IRGS subgroups. Fourth, our findings provided

evidence that the underlying link between IRGS subtypes and reported solid tumors immune classification was well-established. Fifth, the expression of these major immune checkpoints followed the same trend in the IRGS subgroups, the expression levels of *PD-L1, PD-1, CTLA4, LAG3,* and *TIGIT* showed negative correlation to IRGS scores. On the basis of this observation, it is attractive to speculate that patients in the low IRGS group may be more likely to benefit from ICI therapy. Remarkably, this notion could be supported not only by previous reports, but also by our subsequent research results in IPS and IMvigor210 cohort. Moreover, we compared the prognostic ability of IRGS with other two signatures (TIDE and TIS). Ultimately, the IRGS was proven, to act not only a valuable prognostic biomarker, but as an immunotherapeutic indicator for BC patients.

In current paper, we screened eight IFN-γ related genes, including *LATS2, MTHFD2, VAMP8, IRF5, RIPK2, HLA-G, APOL6* and *PTPN6,* and constructed a risk model of BC. Then, RT-qPCR showed that the expression levels of the 6 model genes were significantly different in paired BC and noncancerous tissues (*IRF5, LATS2, MTHFD2, VAMP8, HLA-G* and *PTPN6*). However, the expression of the *RIPK2* and *APOL6* displayed no significant difference between tumor and the matched normal tissues, which may be due to limitations of the quantity of tissues collected (Fig. S7). We next inspected the relationship between the differentially expressed genes in paired tissues and tumor progression or immunity. Large tumor suppressor kinase 2 (*LATS2*) was regarded as a tumor suppressor, and its loss of function may cause activation of oncogenic YAP1/TEAD signaling, which result in a poorer prognosis of urologic cancers patients [58]. As for methylenetetrahydrofolate dehydrogenase (NADP + dependent) 2 (*MTHFD2*), a novel candidate

oncogene in human tumors, it was proved to be as a promising biomarker in BC diagnosis and closely correlated with immune infiltration [59]. Furthermore, a recent study had also confirmed that *MTHFD2* could activate *CDK2* and promote bladder cancer cell growth [60]. Vesicle associated membrane protein 8 (*VAMP8*) had been reported to be associated with chemotherapy resistance in glioma cells, and plays suppressor role in tumor metastasis [61, 62]. In addition, previous studies suggested that Interferon regulatory Factor 5 (*IRF5*) expression correlates with M1/2 macrophages polarization and plays an important role in inflammation, tissue repair and cancer occurrence [63, 64, 65]. Afterwards, major histocompatibility complex, class I, G (*HLA-G*) is one of the "non-classical" HLA antigens (class Ib), which could suppress key immune cells, thus assisting tumors immune escape, and is therefore considered a novel immune checkpoint [66]. Protein tyrosine phosphatase nonreceptor type 6 (*PTPN6*) is a nonreceptor protein tyrosine phosphatase, which may exert its tumor suppressor function through the phosphorylation of carcinogenic kinases [67]. As for BC, *PTPN6* had also been reported to be associated with the tumor immunity and prognosis [68]. In summary, these data markedly demonstrated the feasibility of developing a risk model with above IFN-γ related genes and suggested that the IRGS was a promising biomarker associated with tumor immunity.

Intratumoral BC microenvironment factors, especially those induced by tumor cells and those induced by the TME in response to tumor signaling, was a prominent driver of BC progression, and might be potential intervention targets to facilitate the positive outcome. Recently, the immune cells, as the critical component of the TME had been reported to be related to cancer progression and prognosis [69, 70]. For instance, dense infiltration of CD8 T cells could mediate a durable antitumor response and contribute to improved prognosis [71, 72, 73]. Generally speaking, M2 macrophages, the most frequently observed macrophages subtype in the TME, induce an immunotolerant and pro-tumorigenic microenvironment, and M2 macrophages infiltration levels has already proved to be an adverse prognostic factor for breast, bladder, ovarian, gastric, and prostate cancers [74]. Furthermore, the latest research suggested that overexpression of *HSF1* in BC cells increased M2 TAMs recruitment in a CCL20-dependent manner, with the possibility to be revelated to the promotion of lymphatic metastasis [75]. Besides, as one of the core components of protective immunity to infection and cancer, dendritic cells activated could enhance cytotoxic T lymphocyte responses and facilitate protective anti-tumor immunity [76, 77]. Our findings were in line with the prior studies that higher levels of CD8 T cells and dendritic cells activated were associated low IRGS group with better prognosis, while higher levels of M2 macrophages were associated high IRGS group with poorer prognosis. Noteworthy, the link between IRGS subtypes and reported solid tumors immune classification revealed that the high IRGS group possesses more C1, while the low IRGS group possesses more C3. Researches suggested that solid tumors of immune classification C1 was associated with higher rate of proliferation and poor prognosis, the opposite was true for solid tumors of immune classification C3 [38]. Our results were consistent with this point that the high IRGS group had a poorer OS than that in the low IRGS group. Meanwhile, GSVA and GSEA results inferred that tumor-progression related pathways (focal adhesion, ECM-receptor interaction, WNT/β-catenin, TGF-β, KRAS, and TNFa/NF-kB pathways) predominate in the high IRGS group. These further proved that high IRGS group was characterized by an active tumor aggressiveness. In general, above findings implied that the prognostic value of IRGS might derive from stronger immunosuppression or more malignant tumor growth.

It is generally known that awareness on what causes affect immunotherapy responses is the key to further promote tumor immunotherapy. Previous studies gave some insight into this question. For example, there were researches pointing out that the component of the TIME is a decisive factor of tumor–immune interactions and can influence immunotherapeutic responses [78]. To be specific, a clinical experiment proved that patients with dense CD8+T cells infiltration show higher responsivity to pembrolizumab [23]. In addition, recent study has also suggested that mucosal melanoma patients with sparse lymphocytes infiltration tend to benefit less from ICI therapy [24]. Also, it has previously been reported that BC patients with higher immune checkpoint expression gained more benefit of ICI compared to BC patients with low immune checkpoint expression [49]. Thus, we could summarize that patient with dense lymphocytes infiltration and high expression levels of immune checkpoint molecules tend to benefit more from ICI therapy. In this research, the low IRGS group showed higher expression levels of immune checkpoint molecules, denser CD8+T cells infiltration, and more benefit from ICI treatment compared with the high IRGS group. Therefore, superior response to ICI of the low IRGS group might derive from the favorable immune microenvironment and high expression levels of immune checkpoint molecules.

However, it is necessary to mention that there are some shortcomings to be pointed out with this study. First, the regarding mechanisms of the IRGS subgroups require vitro or vivo experiments to clarify. Second, the reliability of the IRGS needs to be further verified in other cohorts and prospective study.

5. Conclusion

Our study developed an interferon-γ related gene signature on the basis of the eight genes (*LATS2, MTHFD2, VAMP8, IRF5, RIPK2, HLA-G, APOL6* and *PTPN6*), which could serve as an indicator for the prognosis and immunotherapy benefit in bladder cancer.

Declarations

Author contribution statement

Jirong Wang: Performed the experiments; Wrote the paper.
Siyu Chen; Xinpeng Fan: Analyzed and interpreted the data.
Huabin Wang; Jinlong Cao; Jiangwei Man; Qingchao Li: Contributed reagents, materials, analysis tools or data.
Li Yang: Conceived and designed the experiments.

Data availability statement

Data will be made available on request.

Declaration of interest's statement

The authors declare no competing interests.

Additional information

Supplementary content related to this article has been published online at https://doi.org/10.1016/j.heliyon.2022.e12102.

References

[1] H. Sung, J. Ferlay, R.L. Siegel, et al., Global cancer statistics 2020: GLOBOCAN estimates of incidence and mortality worldwide for 36 cancers in 185 countries, CA A Cancer J. Clin. 71 (3) (2021) 209–249.

[2] J. Ferlay, M. Colombet, I. Soerjomataram, et al., Estimating the global cancer incidence and mortality in 2018: GLOBOCAN sources and methods, Int. J. Cancer 144 (8) (2019) 1941–1953.

[3] P.J. Gray, S.A. Fedewa, Shipley Wu, et al., Use of potentially curative therapies for muscle-invasive bladder cancer in the United States: results from the National Cancer Data Base, Eur. Urol. 63 (5) (2013) 823–829.

[4] J.L. Gore, M.S. Litwin, J. Lai, et al., Use of radical cystectomy for patients with invasive bladder cancer, J. Natl. Cancer Inst. 102 (11) (2010) 802–811.

[5] X. Chen, J. Zhang, W. Ruan, et al., Urine DNA methylation assay enables early detection and recurrence monitoring for bladder cancer, J. Clin. Invest. 130 (12) (2020) 6278–6289.

[6] S. Antoni, J. Ferlay, I. Soerjomataram, A. Znaor, A. Jemal, F. Bray, Bladder cancer incidence and mortality: a global overview and recent trends, Eur. Urol. 71 (1) (2017) 96–108.

[7] A.K. Schneider, M.F. Chevalier, L. Derré, The multifaceted immune regulation of bladder cancer, Nat. Rev. Urol. 16 (10) (2019) 613–630.

[8] J. Alfred Witjes, T. Lebret, E.M. Comperat, et al., Updated 2016 EAU guidelines on muscle-invasive and metastatic bladder cancer, Eur. Urol. 71 (3) (2017) 462–475.

[9] J.P. Stein, D.G. Skinner, Radical cystectomy for invasive bladder cancer: long-term results of a standard procedure, World J. Urol. 24 (3) (2006) 296–304.

[10] A. Pearce, M. Haas, R. Viney, et al., Incidence and severity of self-reported chemotherapy side effects in routine care: a prospective cohort study, PLoS One 12 (10) (2017), e0184360.

[11] M. Di Maio, E. Basch, J. Bryce, F. Perrone, Patient-reported outcomes in the evaluation of toxicity of anticancer treatments, Nat. Rev. Clin. Oncol. 13 (5) (2016) 319–325.

[12] S. Antoni, J. Ferlay, I. Soerjomataram, A. Znaor, A. Jemal, F. Bray, Bladder cancer incidence and mortality: a global overview and recent trends, Eur. Urol. 71 (1) (2017) 96–108.

[13] N.M. Donin, A.T. Lenis, S. Holden, et al., Immunotherapy for the treatment of urothelial carcinoma, J. Urol. 197 (1) (2017) 14–22.

[14] S.L. Topalian, F.S. Hodi, J.R. Brahmer, et al., Safety, activity, and immune correlates of anti-PD-1 antibody in cancer, N. Engl. J. Med. 366 (26) (2012) 2443–2454.

[15] T. Powles, J.P. Eder, G.D. Fine, et al., MPDL3280A (anti-PD-L1) treatment leads to clinical activity in metastatic bladder cancer, Nature 515 (7528) (2014) 558–562.

[16] J. Bellmunt, R. de Wit, D.J. Vaughn, et al., Pembrolizumab as second-line therapy for advanced urothelial carcinoma, N. Engl. J. Med. 376 (11) (2017) 1015–1026.

[17] Y. Zeng, Y. Zeng, H. Yin, et al., Exploration of the immune cell infiltration-related gene signature in the prognosis of melanoma, Aging (Albany NY) 13 (3) (2021) 3459–3482.

[18] C. Camisaschi, V. Vallacchi, C. Castelli, L. Rivoltini, M. Rodolfo, Immune cells in the melanoma microenvironment hold information for prediction of the risk of recurrence and response to treatment, Expert Rev. Mol. Diagn 14 (6) (2014) 643–646.

[19] T.J. Curiel, Regulatory T cells and treatment of cancer, Curr. Opin. Immunol. 20 (2) (2008) 241–246.

[20] M.F. Sanmamed, L. Chen, A Paradigm Shift in Cancer Immunotherapy: From Enhancement to Normalization [published correction appears in Cell. 2019 Jan 24; 176(3):677], Cell 175 (2) (2018) 313–326.

[21] A.C. Huang, M.A. Postow, R.J. Orlowski, et al., T-cell invigoration to tumour burden ratio associated with anti-PD-1 response, Nature 545 (7652) (2017) 60–65.

[22] D.R. Camidge, R.C. Doebele, K.M. Kerr, Comparing and contrasting predictive biomarkers for immunotherapy and targeted therapy of NSCLC, Nat. Rev. Clin. Oncol. 16 (6) (2019) 341–355.

[23] E.B. Garon, M.D. Hellmann, N.A. Rizvi, et al., Five-year overall survival for patients with advanced non–small-cell lung cancer treated with pembrolizumab: results from the phase I KEYNOTE-001 study, J. Clin. Oncol. 37 (28) (2019) 2518–2527.

[24] Y. Nakamura, Z. Zhenjie, K. Oya, et al., Poor lymphocyte infiltration to primary tumors in acral lentiginous melanoma and mucosal melanoma compared to cutaneous melanoma, Front. Oncol. 10 (2020), 524700.

[25] M. Nishino, N.H. Ramaiya, H. Hatabu, F.S. Hodi, Monitoring immune-checkpoint blockade: response evaluation and biomarker development, Nat. Rev. Clin. Oncol. 14 (11) (2017) 655–668.

[26] M.T. Baldridge, K.Y. King, N.C. Boles, D.C. Weksberg, M.A. Goodell, Quiescent haematopoietic stem cells are activated by IFN-gamma in response to chronic infection, Nature 465 (7299) (2010) 793–797.

[27] J.M. Curtsinger, P. Agarwal, D.C. Lins, M.F. Mescher, Autocrine IFN-γ promotes naive CD8 T cell differentiation and synergizes with IFN-α to stimulate strong function, J. Immunol. 189 (2) (2012) 659–668.

[28] O.A. Haabeth, K.B. Lorvik, C. Hammarstrom, et al., Inflammation driven by tumour-specific Th1 cells protects against B-cell cancer, Nat. Commun. 2 (2011) 240.

[29] S.J. Lee, B.C. Jang, S.W. Lee, et al., Interferon regulatory factor-1 is prerequisite to the constitutive expression and IFN-gamma-induced upregulation of B7-H1 (CD274), FEBS Lett. 580 (3) (2006) 755–762.

[30] S.C. Liang, Y.E. Latchman, J.E. Buhlmann, et al., Regulation of PD-1, PD-L1, and PD-L2 expression during normal and autoimmune responses, Eur. J. Immunol. 33 (10) (2003) 2706–2716.

[31] K. Abiko, N. Matsumura, J. Hamanishi, et al., IFN-γ from lymphocytes induces PD-L1 expression and promotes progression of ovarian cancer, Br. J. Cancer 112 (9) (2015) 1501–1509.

[32] E.N. Arwert, E.L. Milford, A. Rullan, et al., STING and IRF3 in stromal fibroblasts enable sensing of genomic stress in cancer cells to undermine oncolytic viral therapy [published correction appears in Nat Cell Biol. 2020 Jun 18], Nat. Cell Biol. 22 (7) (2020) 758–766.

[33] L. Liu, X. Du, J. Fang, et al., Development of an interferon gamma response-related signature for prediction of survival in clear cell renal cell carcinoma, J. Inflamm. Res. 14 (2021) 4969–4985.

[34] B. Yao, L. Wang, H. Wang, et al., Seven interferon gamma response genes serve as a prognostic risk signature that correlates with immune infiltration in lung adenocarcinoma, Aging (Albany NY) 13 (8) (2021) 11381–11410.

[35] C. Gillezeau, N. Movva, M. van Gerwen, et al., Interferon gamma expression and mortality in unselected cohorts of urothelial bladder cancer patients, PLoS One 17 (8) (2022), e0271339.

[36] T. Sakatani, Y. Kita, M. Fujimoto, et al., IFN-gamma expression in the tumor microenvironment and CD8-positive tumor-infiltrating lymphocytes as prognostic markers in urothelial cancer patients receiving pembrolizumab, Cancers 14 (2) (2022) 263.

[37] N. van Dijk, S.A. Funt, C.U. Blank, T. Powles, J.E. Rosenberg, M.S. van der Heijden, The cancer immunogram as a framework for personalized immunotherapy in urothelial cancer, Eur. Urol. 75 (3) (2019) 435–444.

[38] V. Thorsson, D.L. Gibbs, S.D. Brown, et al., The immune landscape of cancer [published correction appears in immunity. 2019 Aug 20;51(2):411-412], Immunity 48 (4) (2018) 812–830, e14.

[39] T.M. Malta, A. Sokolov, A.J. Gentles, et al., Machine learning identifies stemness features associated with oncogenic dedifferentiation, Cell 173 (2) (2018) 338–354, e15.

[40] A. Rody, U. Holtrich, L. Pusztai, et al., T-cell metagene predicts a favorable prognosis in estrogen receptor-negative and HER2-positive breast cancers, Breast Cancer Res. 11 (2) (2009) R15.

[41] P. Jiang, S. Gu, D. Pan, et al., Signatures of T cell dysfunction and exclusion predict cancer immunotherapy response, Nat. Med. 24 (10) (2018) 1550–1558.

[42] M. Ayers, J. Lunceford, M. Nebozhyn, et al., IFN-γ-related mRNA profile predicts clinical response to PD-1 blockade, J. Clin. Invest. 127 (8) (2017) 2930–2940.

[43] G.P. Dunn, A.T. Bruce, H. Ikeda, L.J. Old, R.D. Schreiber, Cancer immunoediting: from immunosurveillance to tumor escape, Nat. Immunol. 3 (11) (2002) 991–998.

[44] A. Agarwal, M. Rani, G.K. Saha, et al., Disregulated expression of the Th2 cytokine gene in patients with intraoral squamous cell carcinoma, Immunol. Invest. 32 (1-2) (2003) 17–30.

[45] I. Eke, N. Cordes, Focal adhesion signaling and therapy resistance in cancer, Semin. Cancer Biol. 31 (2015) 65–75.

[46] J. Brabek, C.T. Mierke, D. Rosel, P. Vesely, B. Fabry, The role of the tissue microenvironment in the regulation of cancer cell motility and invasion, Cell Commun. Signal. 8 (22) (2010).

[47] N. Ready, M.D. Hellmann, M.M. Awad, et al., First-line nivolumab plus ipilimumab in advanced non-small-cell lung cancer (CheckMate 568): outcomes by programmed death ligand 1 and tumor mutational burden as biomarkers, J. Clin. Oncol. 37 (12) (2019) 992–1000.

[48] M.M.S. Balla, H.D. Yadav, B.N. Pandey, Tumorsphere assay provides a better in vitro method for cancer stem-like cells enrichment in A549 lung adenocarcinoma cells, Tissue Cell 60 (2019) 21–24.

[49] T. Powles, P.H. O'Donnell, C. Massard, et al., Efficacy and safety of durvalumab in locally advanced or metastatic urothelial carcinoma: updated results from a phase 1/2 open-label study, JAMA Oncol. 3 (9) (2017), e172411.

[50] P. Charoentong, F. Finotello, M. Angelova, et al., Pan-cancer immunogenomic analyses reveal genotype-immunophenotype relationships and predictors of response to checkpoint blockade, Cell Rep. 18 (1) (2017) 248–262.

[51] S. Yang, Y. Wu, Y. Deng, et al., Identification of a prognostic immune signature for cervical cancer to predict survival and response to immune checkpoint inhibitors, OncoImmunology 8 (12) (2019), e1659094.

[52] R.H. Martinez Rodriguez, O. Buisan Rueda, L. Ibarz, Bladder cancer: present and future. Tumor vesical: presente y futuro, Med. Clin. 149 (10) (2017) 449–455.

[53] M.C. Hall, S.S. Chang, G. Dalbagni, et al., Guideline for the management of nonmuscle invasive bladder cancer (stages Ta, T1, and Tis): 2007 update, J. Urol. 178 (6) (2007) 2314–2330.

[54] T. Seisen, B. Granger, P. Colin, et al., A systematic review and meta-analysis of clinicopathologic factors linked to intravesical recurrence after radical nephroureterectomy to treat upper tract urothelial carcinoma, Eur. Urol. 67 (6) (2015) 1122–1133.

[55] J. Zhang, Q. Zhou, K. Xie, et al., Targeting WD repeat domain 5 enhances chemosensitivity and inhibits proliferation and programmed death-ligand 1 expression in bladder cancer, J. Exp. Clin. Cancer Res. 40 (1) (2021) 203.

[56] X. Li, W.K. Wu, R. Xing, et al., Distinct subtypes of gastric cancer defined by molecular characterization include novel mutational signatures with prognostic capability, Cancer Res. 76 (7) (2016) 1724–1732.

[57] W. Choi, A. Ochoa, D.J. McConkey, et al., Genetic alterations in the molecular subtypes of bladder cancer: illustration in the cancer Genome Atlas dataset, Eur. Urol. 72 (3) (2017) 354–365.

[58] B. Cinar, E. Alp, M. Al-Mathkour, et al., The Hippo pathway: an emerging role in urologic cancers, Am J Clin Exp Urol 9 (4) (2021) 301–317. Published 2021 Aug 25.

[59] L. Zhu, X. Liu, W. Zhang, H. Hu, Q. Wang, K. Xu, MTHFD2 is a potential oncogene for its strong association with poor prognosis and high level of immune infiltrates in urothelial carcinomas of bladder, BMC Cancer 22 (1) (2022) 556.

[60] X. Liu, S. Liu, C. Piao, et al., Non-metabolic function of MTHFD2 activates CDK2 in bladder cancer, Cancer Sci. 112 (12) (2021) 4909–4919.

[61] Y. Chen, D. Meng, H. Wang, et al., VAMP8 facilitates cellular proliferation and temozolomide resistance in human glioma cells, Neuro Oncol. 17 (3) (2015) 407–418.

[62] Y.S. Wang, H.T. Tzeng, C.H. Tsai, et al., VAMP8, a vesicle-SNARE required for RAB37-mediated exocytosis, possesses a tumor metastasis suppressor function, Cancer Lett. 437 (2018) 79–88.

[63] T. Ban, G.R. Sato, T. Tamura, Regulation and role of the transcription factor IRF5 in innate immune responses and systemic lupus erythematosus, Int. Immunol. 30 (11) (2018) 529–536.

[64] H. Almuttaqi, I.A. Udalova, Advances and challenges in targeting IRF5, a key regulator of inflammation, FEBS J. 286 (9) (2019) 1624–1637.

[65] T. Krausgruber, K. Blazek, T. Smallie, et al., IRF5 promotes inflammatory macrophage polarization and TH1-TH17 responses, Nat. Immunol. 12 (3) (2011) 231–238.

[66] S. Jasinski-Bergner, M. Eckstein, H. Taubert, et al., The human leukocyte antigen G as an immune escape mechanism and novel therapeutic target in urological tumors, Front. Immunol. 13 (2022), 811200.

[67] C.Y. Liu, J.C. Su, T.T. Huang, et al., Sorafenib analogue SC-60 induces apoptosis through the SHP-1/STAT3 pathway and enhances docetaxel cytotoxicity in triple-negative breast cancer cells, Mol Oncol 11 (3) (2017) 266–279.

[68] C. Shen, J. Liu, J. Wang, X. Yang, H. Niu, Y. Wang, The analysis of PTPN6 for bladder cancer: an exploratory study based on TCGA, Dis. Markers 2020 (2020), 4312629.

[69] C.L. Zindl, D.D. Chaplin, Immunology. Tumor immune evasion, Science 328 (5979) (2010) 697–698.

[70] I. Milo, M. Bedora-Faure, Z. Garcia, et al., The immune system profoundly restricts intratumor genetic heterogeneity, Sci Immunol 3 (29) (2018), eaat1435.

[71] G. Bindea, B. Mlecnik, M. Tosolini, et al., Spatiotemporal dynamics of intratumoral immune cells reveal the immune landscape in human cancer, Immunity 39 (4) (2013) 782–795.

[72] W.H. Fridman, L. Zitvogel, C. Sautes-Fridman, G. Kroemer, The immune contexture in cancer prognosis and treatment, Nat. Rev. Clin. Oncol. 14 (12) (2017) 717–734.

[73] A.J. Gentles, A.M. Newman, C.L. Liu, et al., The prognostic landscape of genes and infiltrating immune cells across human cancers, Nat. Med. 21 (8) (2015) 938–945.

[74] B. Ruffell, L.M. Coussens, Macrophages and therapeutic resistance in cancer, Cancer Cell 27 (4) (2015) 462–472.

[75] M. Huang, W. Dong, R. Xie, et al., HSF1 facilitates the multistep process of lymphatic metastasis in bladder cancer via a novel PRMT5-WDR5-dependent transcriptional program, Cancer Commun. 42 (5) (2022) 447–470.

[76] D. Alvarez, E.H. Vollmann, U.H. von Andrian, Mechanisms and consequences of dendritic cell migration, Immunity 29 (3) (2008) 325–342.

[77] D. Zhivaki, F. Borriello, O.A. Chow, et al., Inflammasomes within hyperactive murine dendritic cells stimulate long-lived T cell-mediated anti-tumor immunity, Cell Rep. 33 (7) (2020), 108381.

[78] E. Hirata, E. Sahai, Tumor microenvironment and differential responses to therapy, Cold Spring Harb Perspect Med 7 (7) (2017), a026781.